MAIDESC M42, mai 2017

A priori error-based mesh adaptation in CFD

E. Gauci*, A. Belme**, A. Carabias***,
A. Loseille*, F. Alauzet*,***, A. Dervieux*,***

* INRIA, Sophia-Antipolis/Saclay, France,
** UPMC, Paris, France
*** Lemma, Biot, France

MAIDESC M42: AGENDA

Accueil 9:00 café
Début 9:30
E. Hachem Titre non parvenu
Y. Mesri Titre non parvenu
A. Boilley Maillage d'objets complexes avec couche limite
E. Gauci Adaptation ALE
12:00 Repas salle club
Début seconde session 13:30
B. Koobus Progrès en multi-rate
O. Allain Progrès en adaptation
A. Dervieux Exposé de C. Dobrzynski:
An immersed boundary method for NS equations on unstructured anisotropic mesh
A. Dervieux Adaptation basée erreur pour Navier-Stokes

Error reduction

Several approaches for evaluating the effect of an anisotropic mesh change on the final approximation error $u - u_h$:

Apply local deformations:
- A priori estimates.

Formaggia, Perotto,...
- Local discrete perturbation.

Yano, Darmofal.

Our proposition: express the approximation error in terms of interpolation errors.

Overview

- Three families of adaptation criteria (elliptic case)
  - Feature-based (or Hessian-based)
  - Goal-oriented
  - Norm-oriented
- Application to Euler, Navier-Stokes
- Higher-order, unsteady case

I. Feature-based mesh adaptation

Mesh parameterization

Metric $\mathscr{M}$:

$$\mathscr{M}(\mathbf{x}) = \mathscr{R}^t(x,y) \begin{pmatrix} \frac{1}{\Delta\xi^2(x,y)} & 0 \\ 0 & \frac{1}{\Delta\eta^2(x,y)} \end{pmatrix} \mathscr{R}(x,y)$$

$\Delta\xi(x,y), \Delta\eta(x,y)$: mesh sizes in characteristic directions.

$\mathscr{R}(x,y)$ = matrix of eigenvectors.

Number of vertices: $\mathscr{C}(\mathscr{M}) = \int_\Omega \sqrt{det(\mathscr{M}(\mathbf{x}))}\, \mathrm{d}\mathbf{x}$

Which mesh?

A **unit mesh for $\mathscr{M}$** has *any* edge ij of length 1:

$$dist_{\mathscr{M}}(\mathbf{x}_i, \mathbf{x}_j) \doteqdot \int_0^1 \sqrt{{}^t\mathbf{x}_i\mathbf{x}_j \mathscr{M}(\mathbf{x}_i + \theta\mathbf{x}_i\mathbf{x}_j)\mathbf{x}_i\mathbf{x}_j}\, \mathrm{d}\theta \;=\; 1.$$

Feature-based mesh adaptation

Minimize the P^1 **interpolation error** in L^p:

$$\varepsilon^p_{\mathscr{M}} = ||u - \Pi_{\mathscr{M}} u||^p_{L^p} \approx \int_\Omega [\mathrm{trace}(\mathscr{M}^{-\frac{1}{2}}(\mathbf{x})\,|H_u(\mathbf{x})|\,\mathscr{M}^{-\frac{1}{2}}(\mathbf{x}))]^p \mathrm{d}\mathbf{x}$$

under the constraint: $\mathscr{C}(\mathscr{M}) = N$.

H_u is the Hessian matrix of u.

(...magic wand...) $\Leftrightarrow$ **optimal metric field :**

$$\mathscr{M}_{L^p,opt}(\mathbf{x}) = \mathscr{K}_p(1, H^{(*)}_{u_{\mathscr{M}}})$$

$$\mathscr{K}_p(k, H_{u_{\mathscr{M}}}) = \mathscr{D}_{L^p}\ det(|kH_{u_{\mathscr{M}}}(\mathbf{x})|)^{\frac{-1}{2p+dim}}\ |kH_{u_{\mathscr{M}}}(\mathbf{x})|$$

$$\mathscr{D}_{L^p} = N^{\frac{2}{dim}} \left(\int_\Omega det(|kH_{u_{\mathscr{M}}}(\mathbf{x})|)^{\frac{p}{2p+dim}}\ \mathrm{d}\mathbf{x}\right)^{-\frac{2}{dim}} \quad (\text{here } dim = 2).$$

(*): evaluated by **recovery**.

Application of feature-based to a simulation

Step 1: solve PDE for *state* $u_{\mathscr{M}}$,
Step 2: evaluate $\mathscr{M}_{L^p,opt}$,
Step 3: build new unit mesh for $\mathscr{M}_{L^p,opt}$; go to 1.

The main *a priori* limitation of a feature-based method is the delicate choice of the feature(s) (="sensor"), in particular for systems.

Further, the feature-based method doesn't take into account the state PDE (only sensors from the solution). In particular, reducing the L^2 interpolation error does reduce as much the approximation error.

Example : Poisson problem with 1D boundary layer as solution.

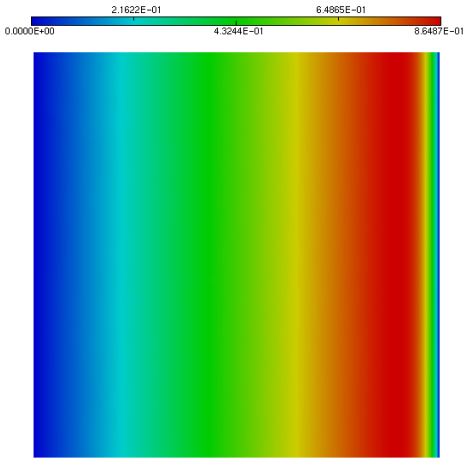
2.1622E-01
6.4865E-01
0.0000E+00
4.3244E-01
8.6487E-01

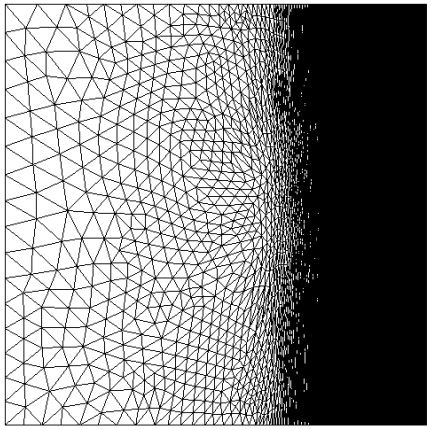

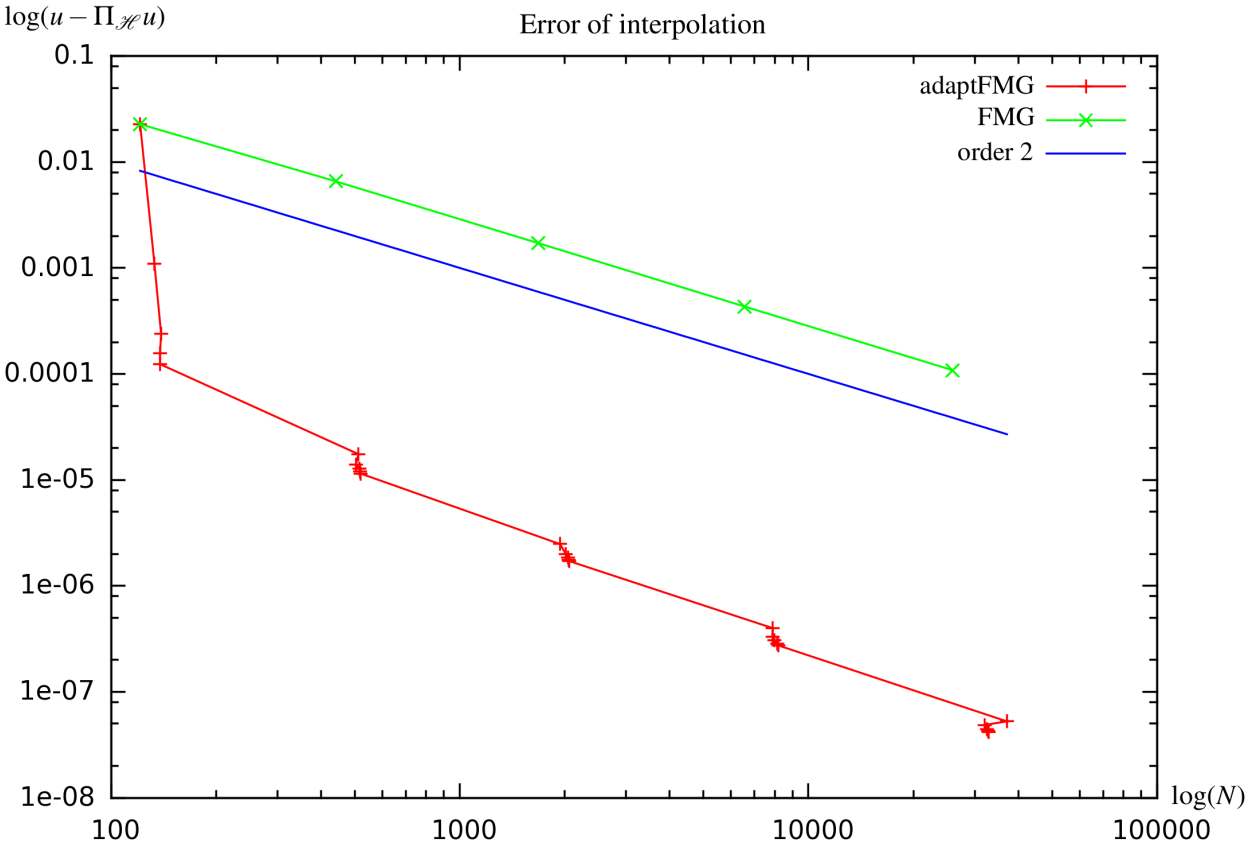
Error of interpolation
log(u − Π_ℋ u)
0.1
0.01
0.001
0.0001
1e-05
1e-06
1e-07
1e-08
100
1000
10000
100000
log(N)
adaptFMG
FMG
order 2

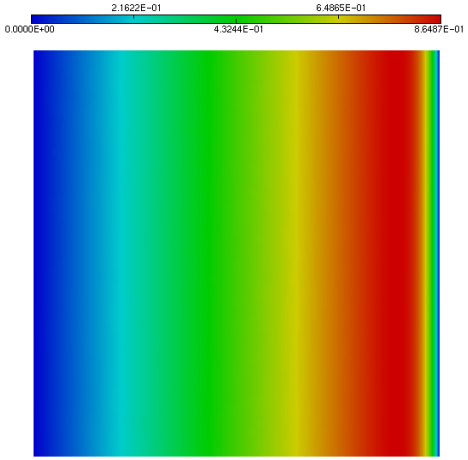
2.1622E-01
6.4865E-01
0.0000E+00
4.3244E-01
8.6487E-01

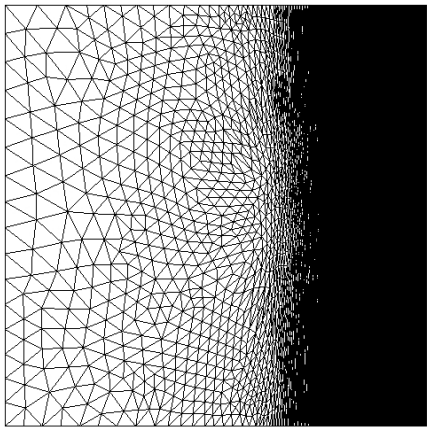

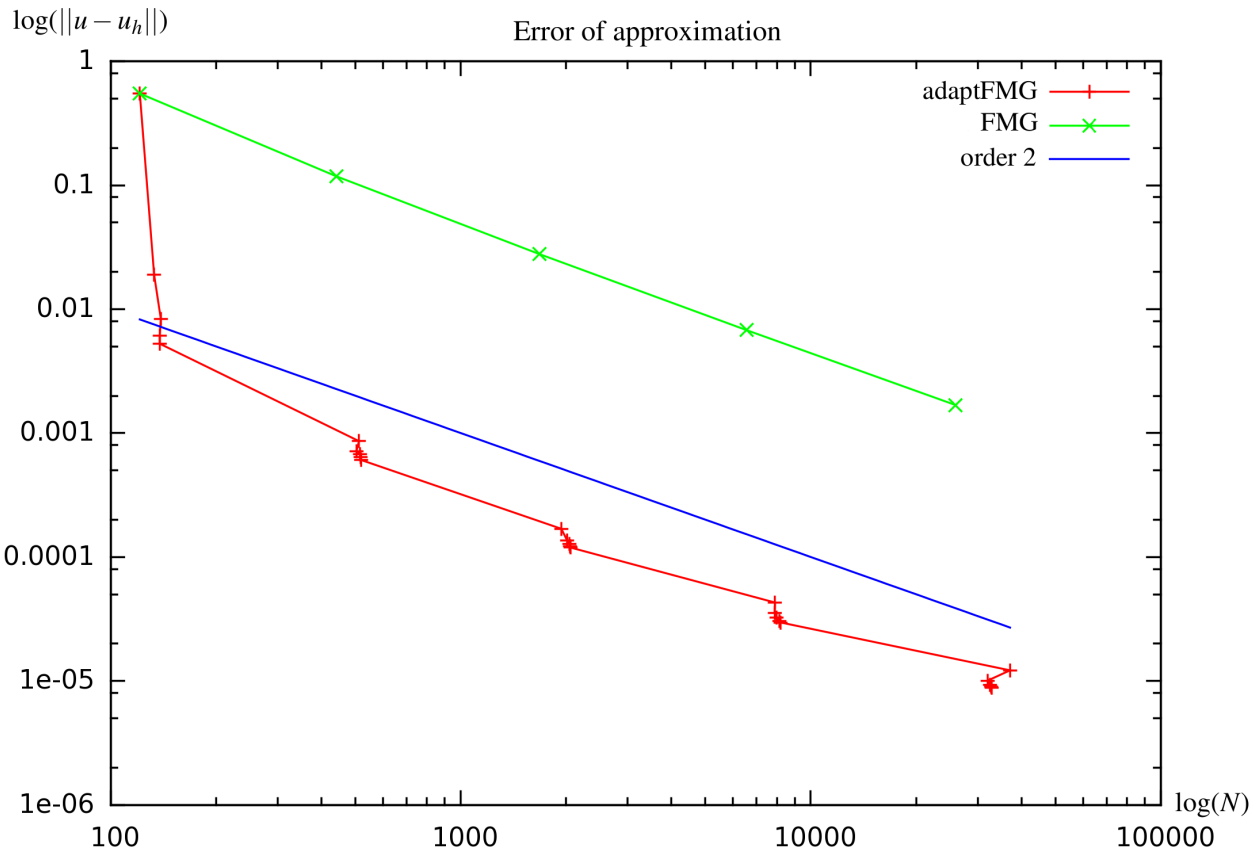
Error of approximation
log(||u − u_h||)
log(N)
adaptFMG
FMG
order 2
1
0.1
0.01
0.001
0.0001
1e-05
1e-06
100
1000
10000
100000

II.Goal-Oriented mesh adaptation

The goal-oriented formulation is probably the first formulation in which the mesh adaptation problem is completely set on a rigorous mathematical form:
Find the mesh which minimizes the approximation error committed on a specified scalar output (g,u)*:*

$$\min_{\mathscr{M}} \delta j_{goal}(\mathscr{M}) = |(g, u - u_{\mathscr{M}})| \ , \ \mathscr{C}(\mathscr{M}) = N$$

$$\Psi(\mathscr{M}, u_{\mathscr{M}}) = 0 \quad , \text{state equation}$$

A. LOSEILLE, A. DERVIEUX and F. ALAUZET, Fully anisotropic goal-oriented mesh adaptation for 3D steady Euler equations, Journal of Computational Physics, Vol. 229, Issue 8, pp. 2866-2897, 2010.

Goal-Oriented mesh adaptation : Poisson problem

State: $\Psi(\mathscr{M}, u_{\mathscr{M}}) = 0 \;\Leftrightarrow\; \Delta u = f, \;\; u|\partial\Omega = 0.$

Adjoint state: $\frac{\partial \Psi}{\partial u}^{*} u^{*} = \frac{\partial J}{\partial u} \quad \Leftrightarrow \; \Delta u^{*} = g, \;\; u^{*}|\partial\Omega = 0$

(...)

$$\mathscr{M}_{opt,goal} = \mathscr{K}_1(|\rho(H(u^{*}_{g,\mathscr{M}}))|, H_{u_{\mathscr{M}}}).$$

$\rho(H(u^{*}_{g,\mathscr{M}}))$: max eigenvalue of Hessian of $u^{*}_{g,\mathscr{M}}$.

Goal-Oriented mesh adaptation (cont'd)

Step 1: solve state
Step 2: solve adjoint state
Step 3: evaluate metric :

$$\mathscr{M}_{opt,goal} = \mathscr{K}_1(|\rho(H(u^*))|, H_u)$$

Step 4: generate unit mesh for $\mathscr{M}_{opt,goal}$. Go to 1.

But:
- only features influencing the scalar functional will be refined,
- then we have lost the convergence to the PDE solution!

Computational example:

Supersonic business aircraft at farfield Mach number 1.6.

Bottom: mesh adaptation based on the feature “Mach number”.

Top: mesh adaptation based on the goal of pressure integral at ground.

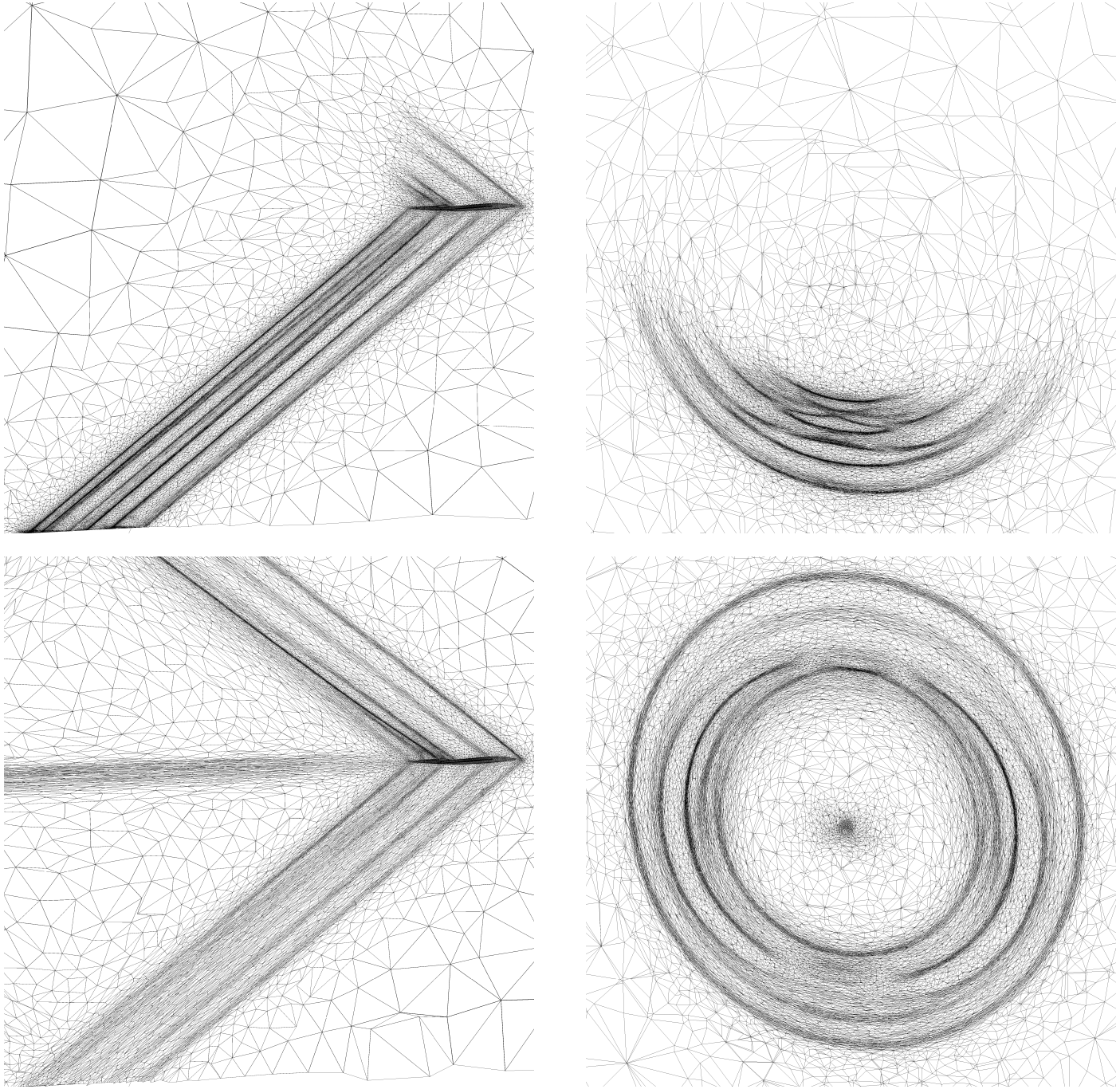

III. Norm-Oriented mesh adaptation

A goal-oriented adaptation method is not field-convergent.

Functionals generally express *mean* properties while many engineering applications are interested in space or time fluctuations.

Why being satisfied with an accurate single scalar output when the numerical methods claims field convergence?

III. Norm-Oriented mesh adaptation

Minimize:

$$j(\mathscr{M}) = ||u - u_{\mathscr{M}}||^2_{L^2(\Omega)}.$$

We evaluate a **corrector** $g_{corr} \approx u - u_{\mathscr{M}}$ by *coarse-fine Defect Correction.*

$$g_{corr} = \frac{4}{3} A_h^{-1} R_{h/2 \to h}(A_{h/2} P_{h \to h/2} u_h - f_{h/2})$$
$$\Rightarrow j(\mathscr{M}) \approx (g_{corr}, u - u_{\mathscr{M}}).$$

Freezing g_{corr}, we get the goal-oriented context:

Adjoint:

$$a(\psi, u^*_{corr}) = (g_{corr}, \psi)$$

Optimal metric:

$$\mathscr{M}_{opt,norm} = \mathscr{K}_1(|\rho(H(u^*_{corr}))|, H_{u_{\mathscr{M}}})$$

Norm-Oriented Adaptation

Step 1: solve state equation

Step 2: solve corrector equation

Step 3: solve adjoint equation

Step 4: evaluate optimal metric :

$$\mathscr{M}_{opt,norm} = \mathscr{K}_1(|\rho(H(u^*_{corr}))|, H_{u_{\mathscr{M}}}).$$

Step 5: generate unit mesh for $\mathscr{M}_{opt,norm}$ and go to 1.

Convergence, in the prescribed norm, towards the PDE solution.

G. Brèthes, A. Dervieux, Anisotropic Norm-Oriented Mesh Adaptation for a Poisson problem, Journal of Computational Physics 322 (2016) 804-826.
A. Loseille, A,. Dervieux, F. Alauzet, Anisotropic Norm-Oriented Mesh Adaptation for a compressible inviscid flow, AIAA paper, 2015-2037

An example : 2D boundary layer, Poisson problem (Formaggia-Perotto-2003 test case)

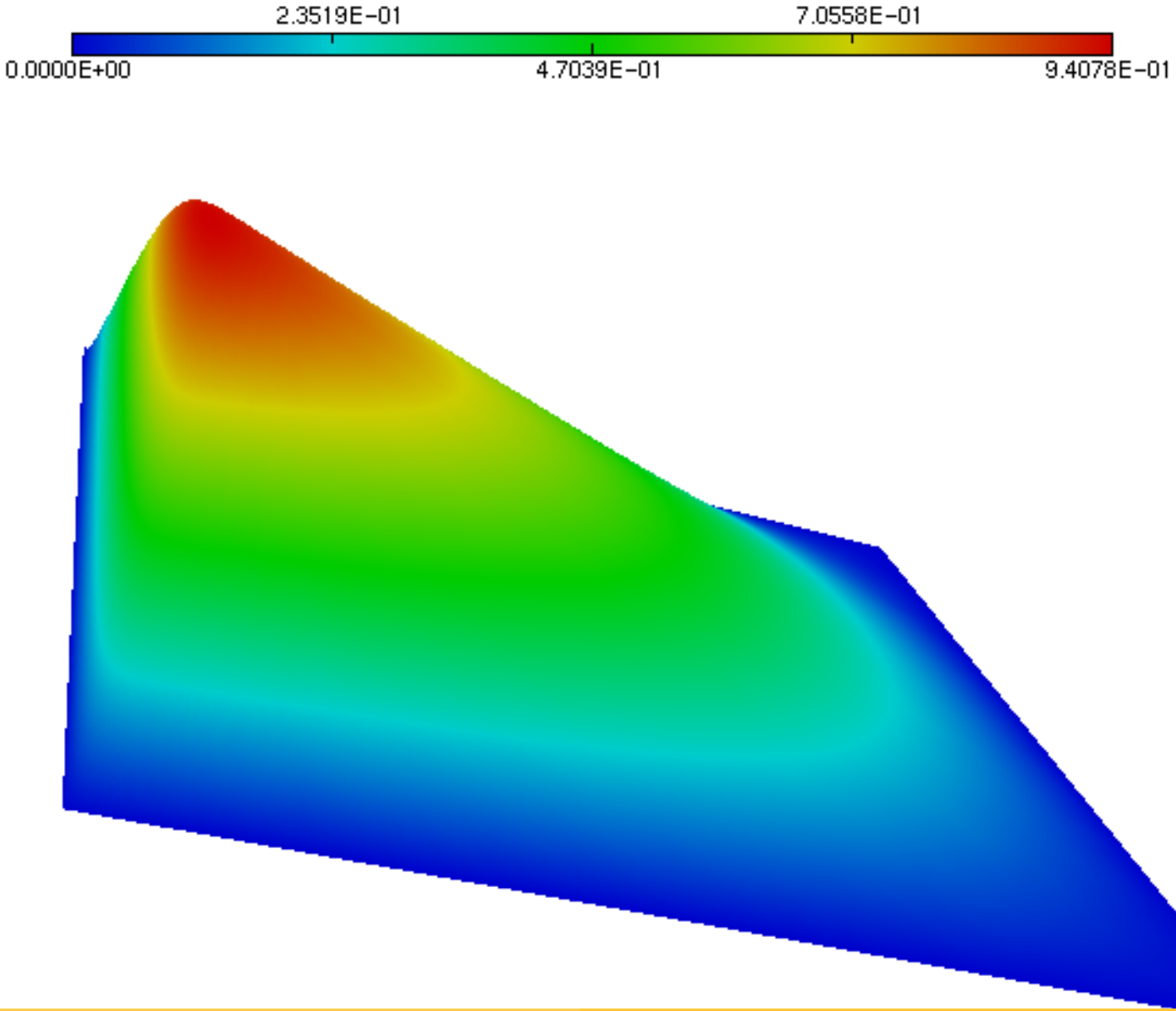

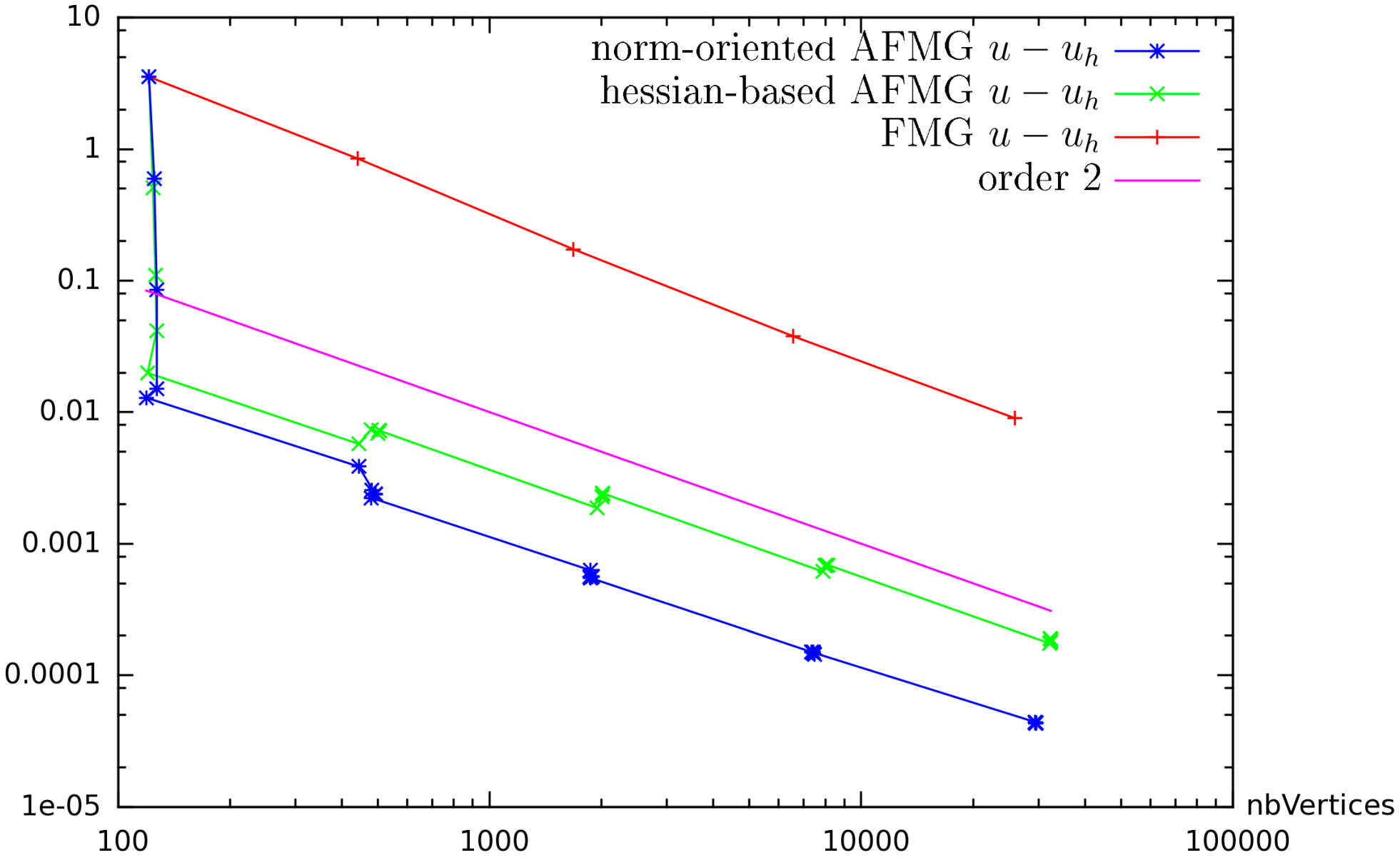
norm-oriented AFMG $u - u_h$
hessian-based AFMG $u - u_h$
FMG $u - u_h$
order 2
10
1
0.1
0.01
0.001
0.0001
1e-05
100
1000
10000
100000
nbVertices

2D boundary layer, cont'd

In practice, we have not $u - u_h$.

We use $u' = g_{coor}$ as an estimate of $u - u_h$.

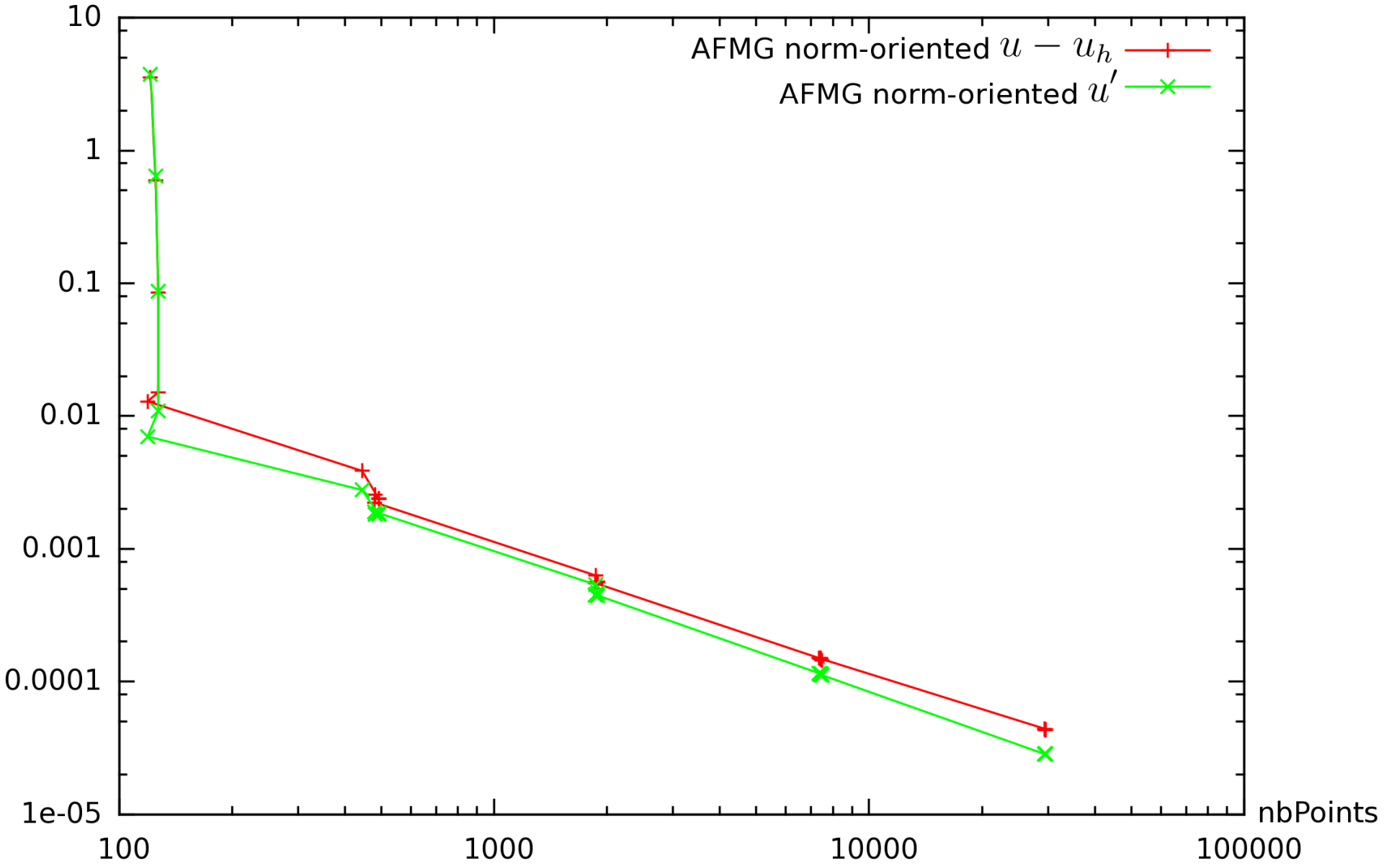
AFMG norm-oriented $u - u_h$
AFMG norm-oriented u'
10
1
0.1
0.01
0.001
0.0001
1e-05
100
1000
10000
100000
nbPoints

Singular test case

Mesh adaptation should manage small scales and singularities.

Example: discontinuous derivative along a curve (in 2D).

Barrier lemma: With adapted anisotropic meshes, convergence can be second-order and not better.

Continuous analysis: It can be shown that:

$$\int_\Omega \det\left(|H_u|\right)^{\frac{p}{2p+dim}} < \infty$$

Then the optimal error is **second-order**:

$$\|u - \pi_{\mathscr{M}_{\mathbf{L}^p}} u\|_{\mathbf{L}^p} \approx N^{-\frac{2}{dim}} \left(\int_\Omega \det\left(|H_u|\right)^{\frac{p}{2p+dim}} \right)^{\frac{2p+dim}{3p}} \leq \frac{\mathbf{Cst}}{\mathbf{N^{2/dim}}}.$$

Solution with a discontinuous gradient

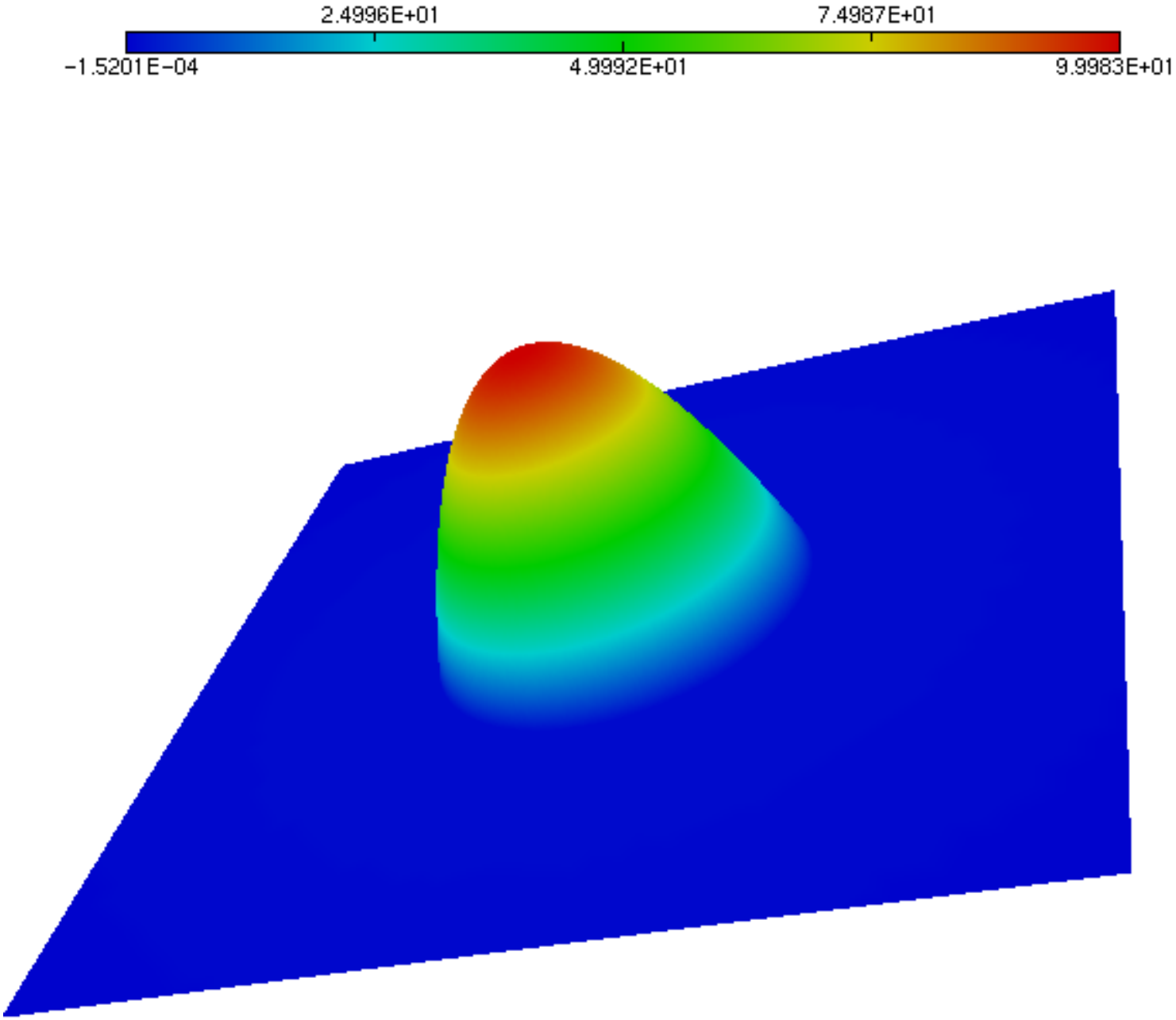

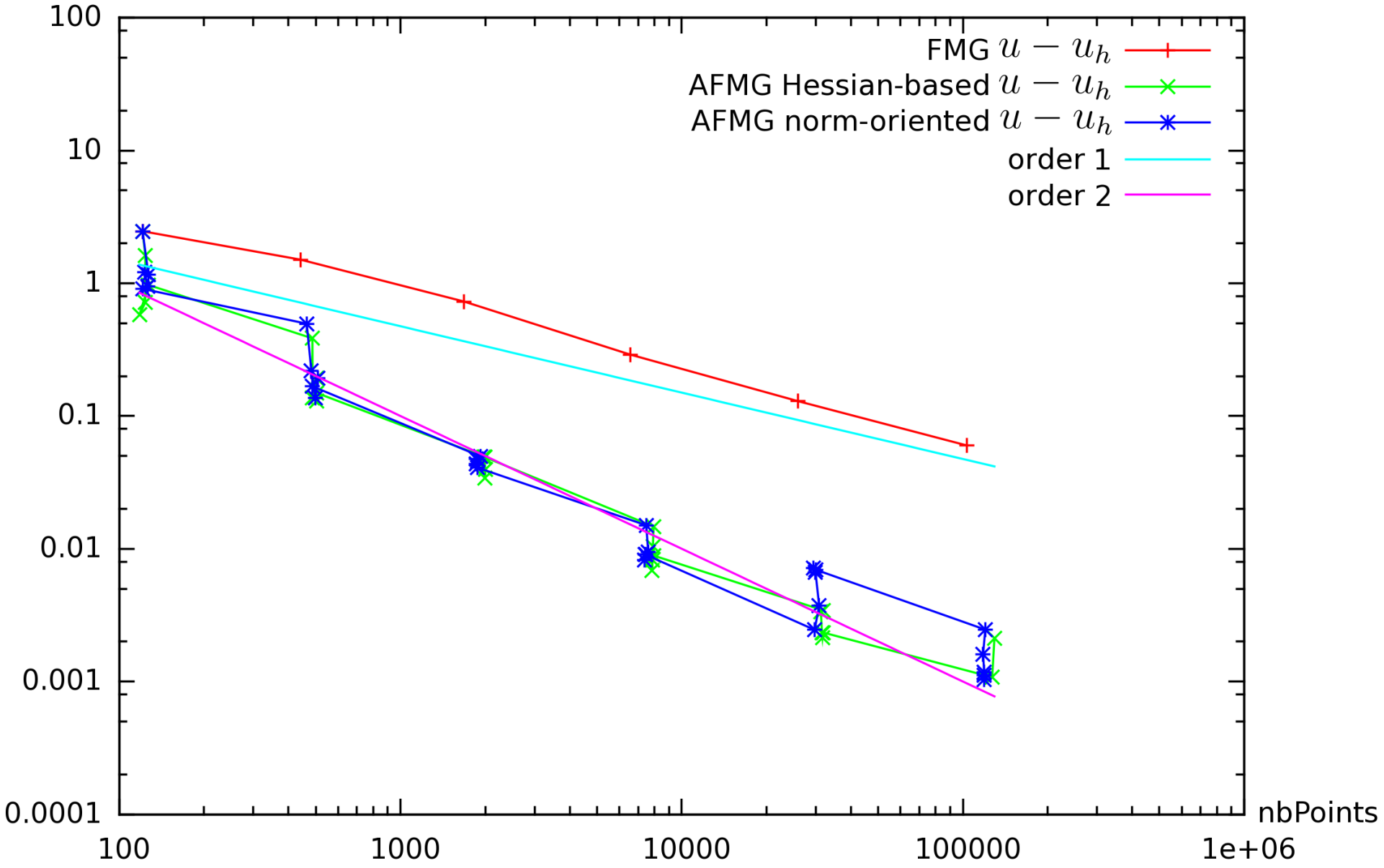
FMG $u - u_h$
AFMG Hessian-based $u - u_h$
AFMG norm-oriented $u - u_h$
order 1
order 2
100
10
1
0.1
0.01
0.001
0.0001
100
1000
10000
100000
1e+06
nbPoints

More complex physics : Euler equations

$$\frac{\partial \mathscr{F}^x(u)}{\partial x} + \frac{\partial \mathscr{F}^y(u)}{\partial y} + \frac{\partial \mathscr{F}^z(u)}{\partial z} = 0 \ + b.\,cond. \Leftrightarrow \Psi^E(u, \mathscr{M}) = 0$$

$$j(\mathscr{M}) = J(u, \mathscr{M}) \ ; \ [\frac{\partial \Psi^E}{\partial u}]^{-*} u^* = \frac{\partial J}{\partial u}$$

(...)

$$\text{Min} \int_\Omega \text{trace}(\mathscr{M}^{-\frac{1}{2}}(\mathbf{x}) \, |\bar{H}(u, u^*)(\mathbf{x})| \, \mathscr{M}^{-\frac{1}{2}}(\mathbf{x}))\mathrm{d}\mathbf{x}$$

$$\bar{H}(u, u^*) = \sum |\frac{\partial u*_j}{\partial x}||H(\mathscr{F}_j^x)| + |\frac{\partial u*_j}{\partial y}||H(\mathscr{F}_j^y)| + |\frac{\partial u*_j}{\partial z}||H(\mathscr{F}_j^z)|$$

Then $\mathscr{M} = \mathscr{K}_1(1, \bar{H})$

Feature-based adaptation for minimizing the L^1 norm of the interpolation error on the density, velocity and pressure.

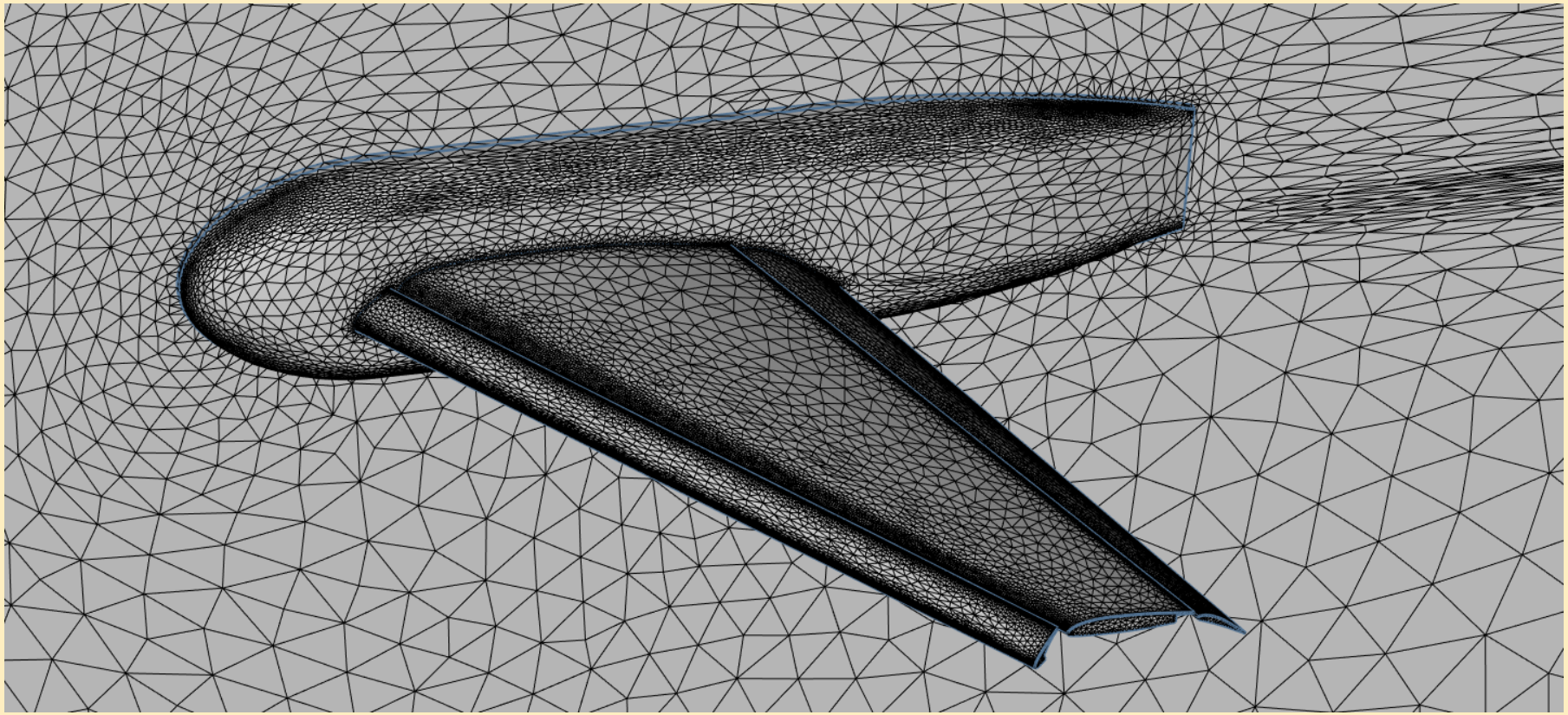

There is not much mesh concentration on the body in the wake of wing.

Feature-based adaptation (cont'd).

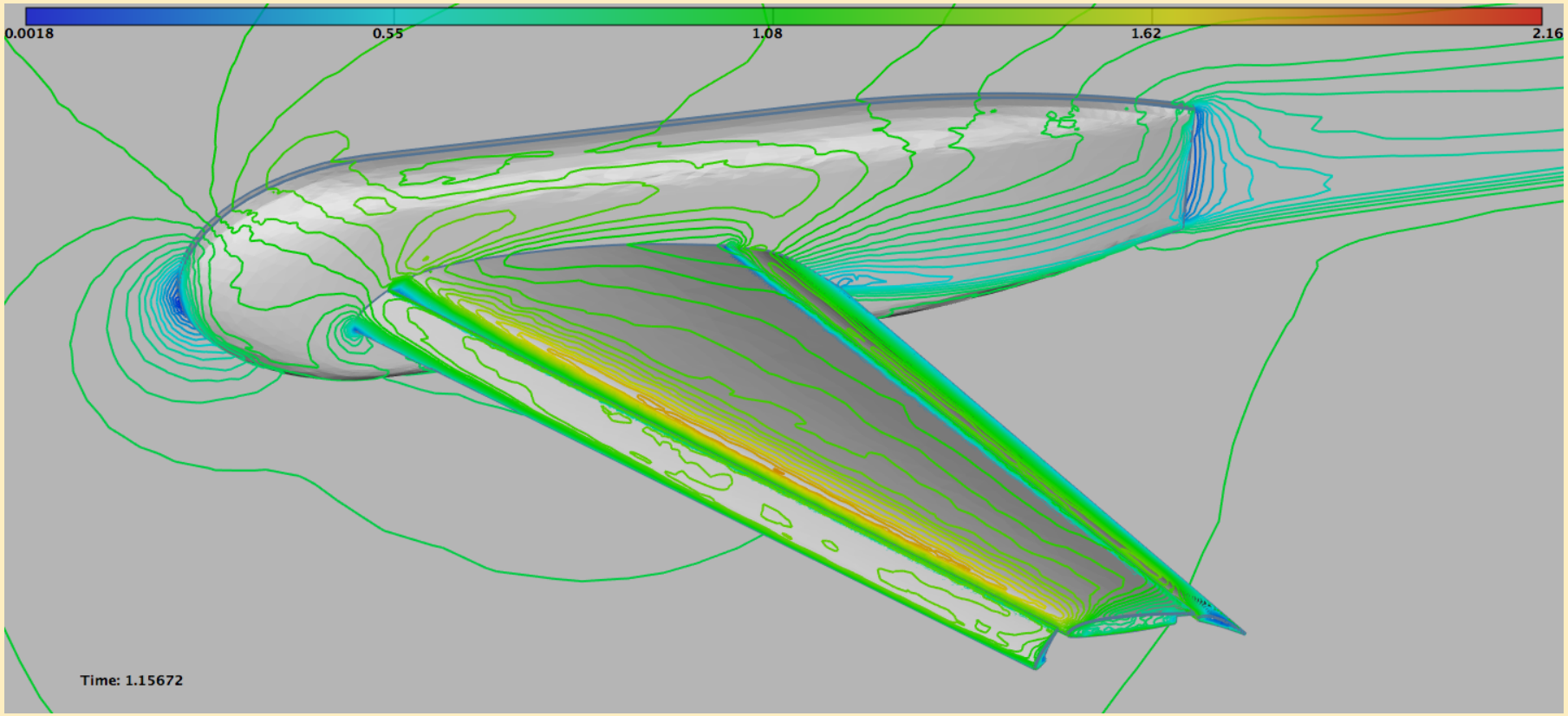

Adaptation for minimizing the norm $||W - Wh||_{L^2}$ with the **norm-oriented** approach.

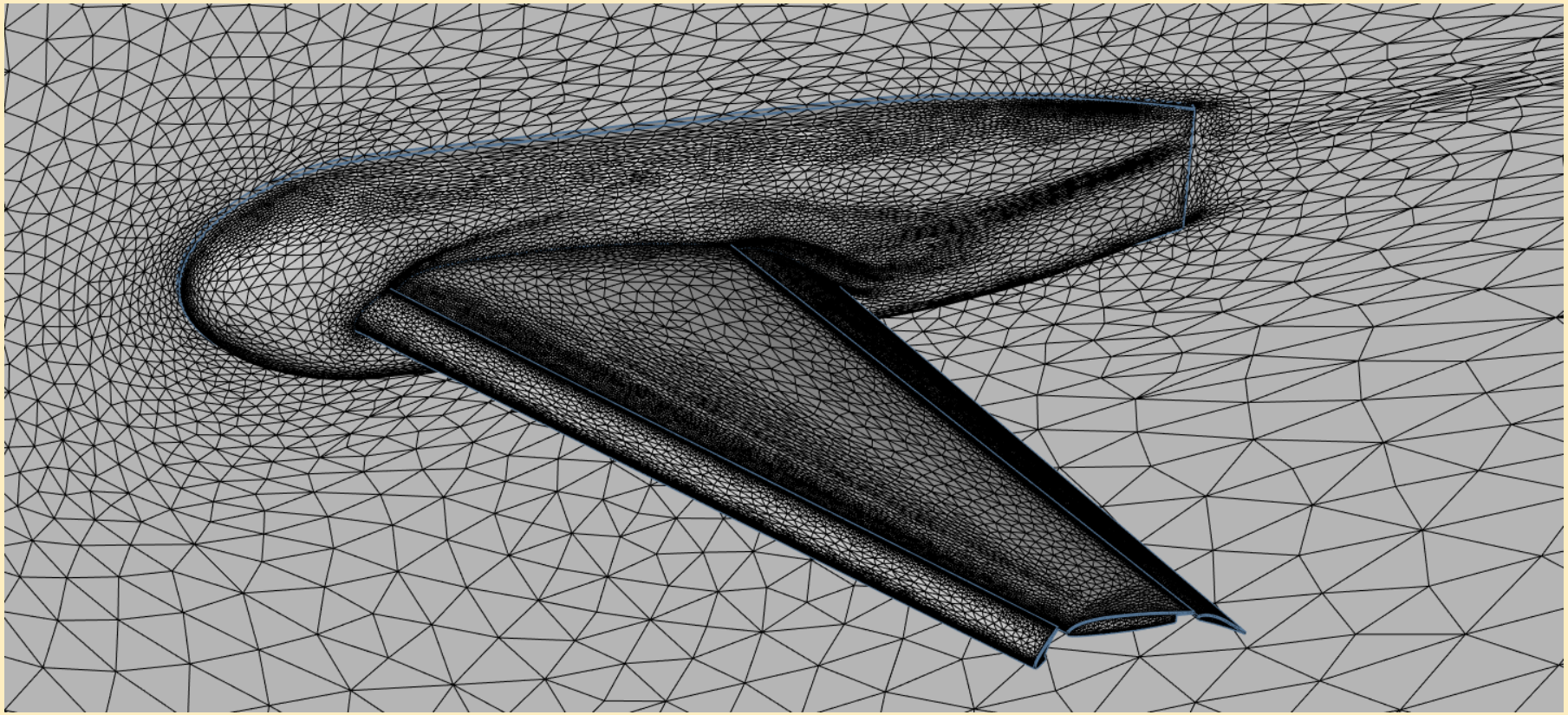

Near-body mesh is finer, and show much more details on the aircraft body.

Norm-oriented, concl'd

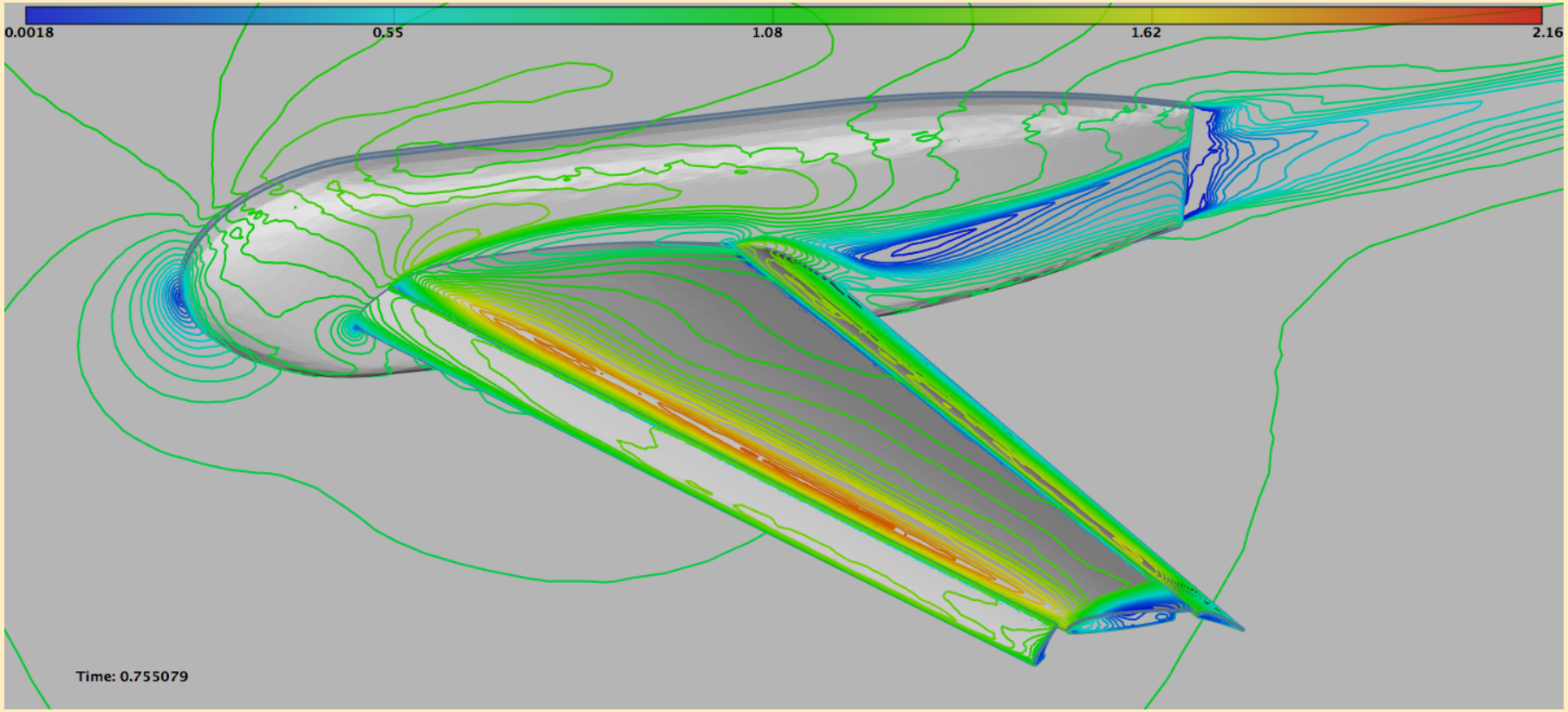

Compressible Navier-Stokes model

$$
\begin{aligned}
(\Psi(W),\Phi) &= \int_{\Omega\times[0,T]} \Phi\, W_t \,\mathrm{d}v\mathrm{d}t \\
-\int_{\Omega\times[0,T]} (\nabla\Phi \cdot \mathscr{F}_E(W) &+ \nabla\Phi \cdot \mathscr{F}_v(W))\mathrm{d}v\mathrm{d}t \\
&+ \int_{\partial\Omega\times[0,T]} \Phi\, \hat{\mathscr{F}}(W)\,\mathrm{d}\sigma\mathrm{d}t
\end{aligned}
$$

$\mathscr{F}_E = [\rho\mathbf{u}, \rho\mathbf{u}\mathbf{u} + p\mathbf{I}, \rho\mathbf{u}H]^T$

$\mathscr{F}_v = [0, \boldsymbol{\sigma}(\nabla\mathbf{u}), -(\mathbf{q}(\lambda\nabla T) - \mathbf{u}.\boldsymbol{\sigma}(\nabla\mathbf{u}))]^T.$

$\boldsymbol{\sigma} = \mu(\nabla\mathbf{u} + \nabla\mathbf{u}^{\mathrm{T}}) - \frac{2}{3}\mu\nabla.\mathbf{u}\mathbf{I}$; $\mathbf{q} = -\lambda\nabla T$

A error analysis applies (similar to elliptic case).

Compressible Navier-Stokes : a 2D example

Flow around a NACA0012,
Mach number $= 1.4$, $\alpha = 0$ deg
Medium Reynolds number: 1000.
Shock reflection on Γ, wall at bottom.

Goal-oriented adaptation with:

$$j = \int_{\Gamma} (p - p_\infty)^2 / p_\infty \mathrm{d}\Gamma.$$

Meshes from 10K to 40K vertices.

2D example (cont'd)

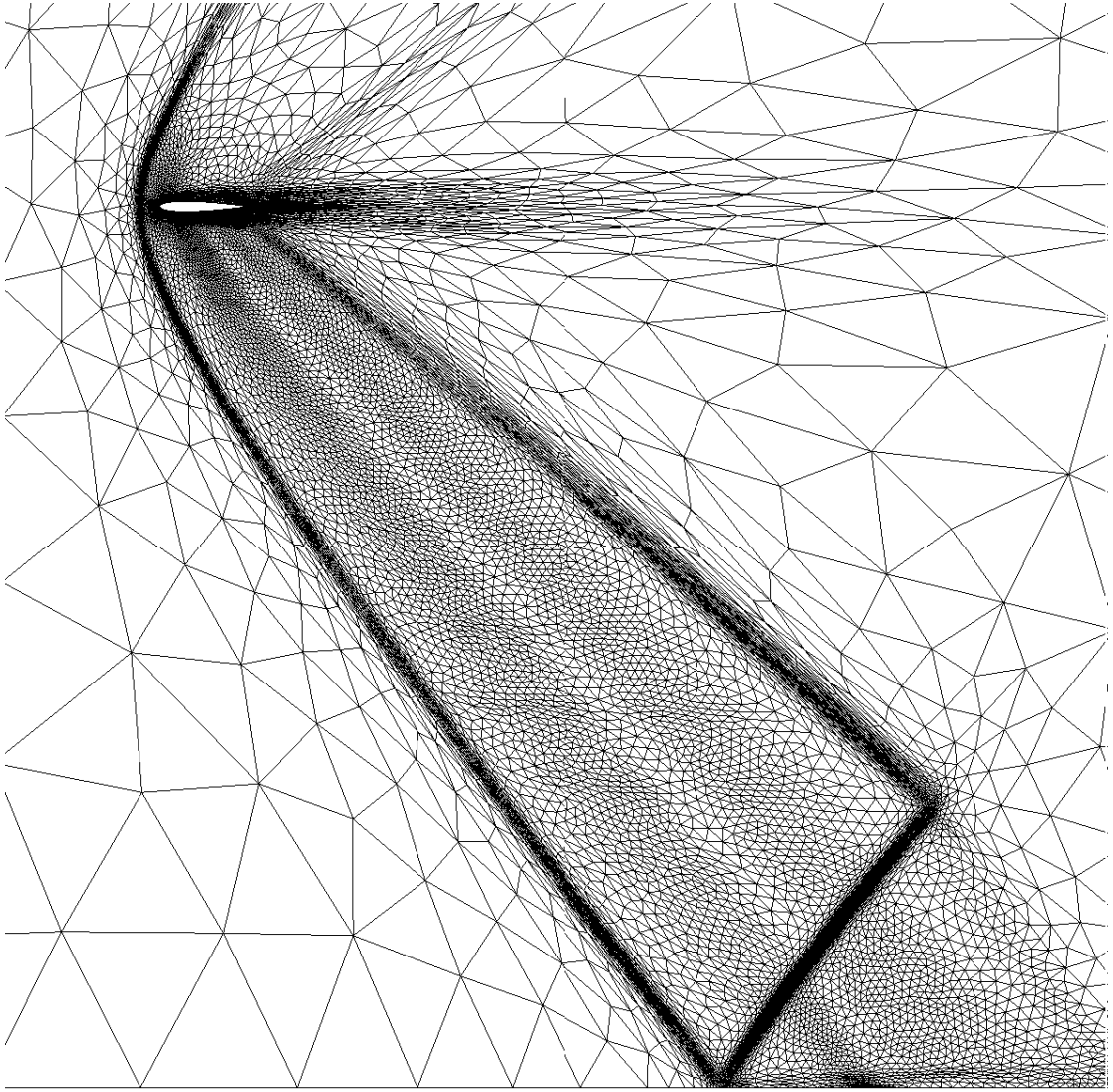

Adaptive mesh for laminar flow with $Rey = 10^3 (20K \text{vertices})$.

2D example (end'd)

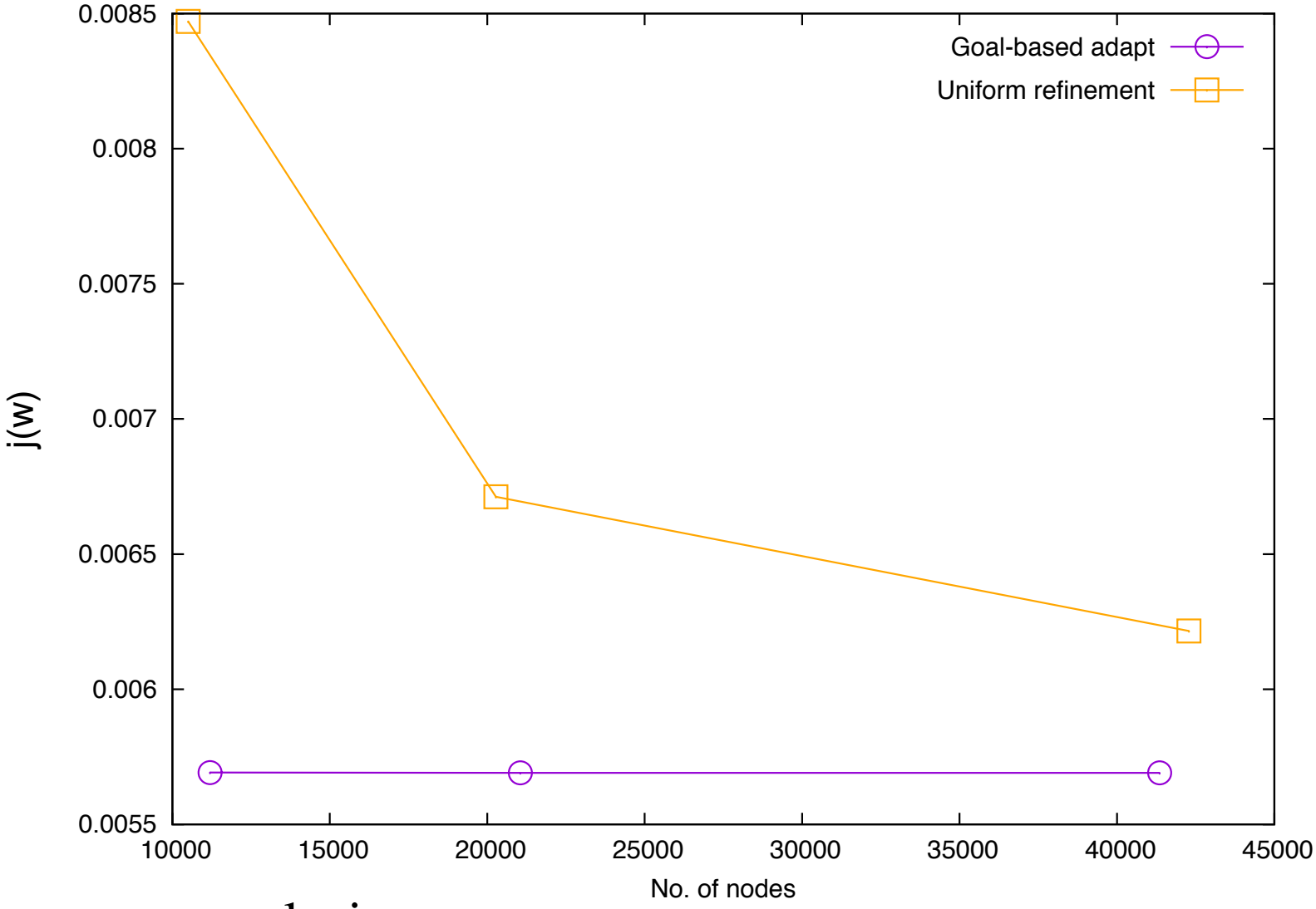

Convergence analysis:

Pressure footprint output functional vs. Mesh size

3D example, turbulent, preliminary

Case : flow around a Falcon aircraft, UMRIDA test case,
Mach number =0.8, $\alpha = 2$ deg.
Spalart Allmaras turbulence model,

Norm-oriented mesh adaptation (except in close boundary layer),

3D example

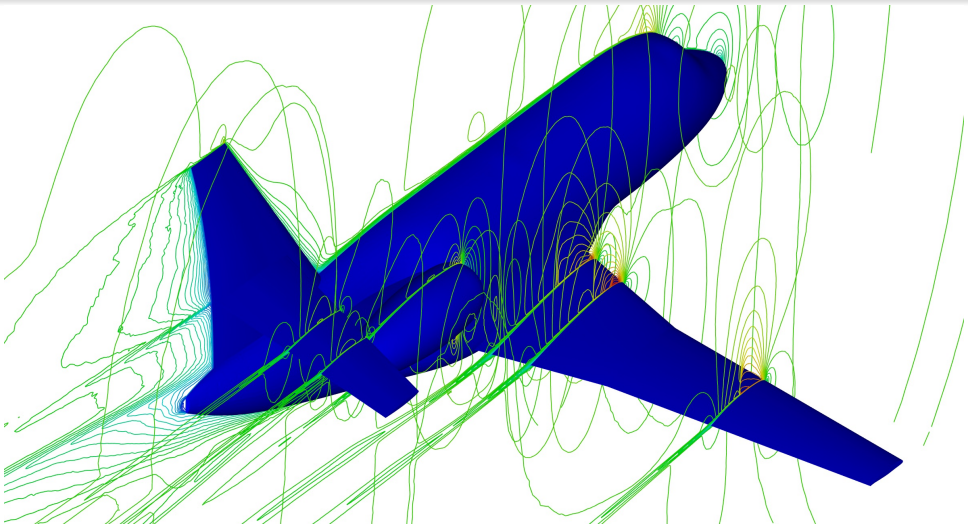

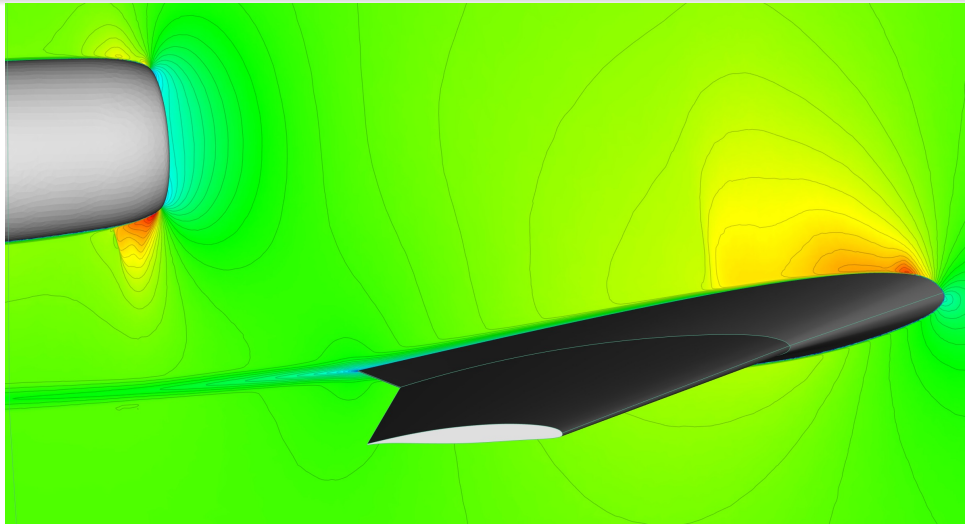

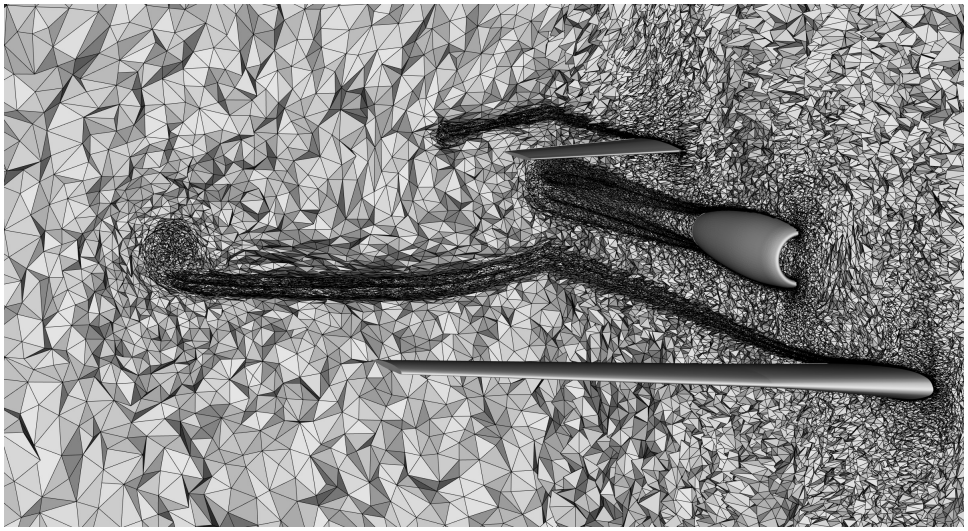

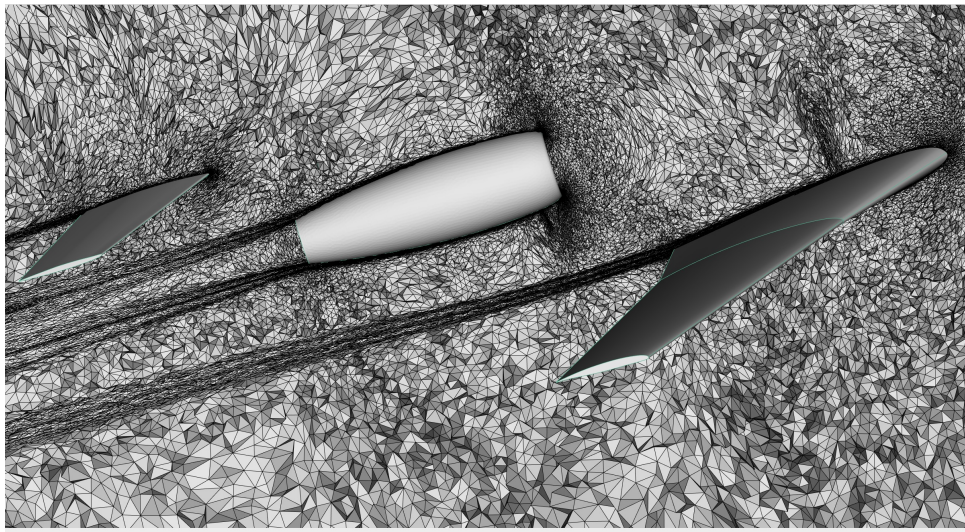

Top, Mach solution field. Bottom, final adapted mesh.

Shape: courtesy of Dassault Aviation.

Compressible Navier-Stokes model (end'd)

- Mesh convergence $\Leftrightarrow$ 415K vertices ("current")
- Comparison with a very fine mesh (10M vertices, "final")
- C_p cut on wing,
- Use of the **corrector** by visualizing:

  $$\text{"pressure } \pm \mid \text{ corrected pressure} - \text{pressure } \mid\text{"}$$

  for estimating the accuracy.

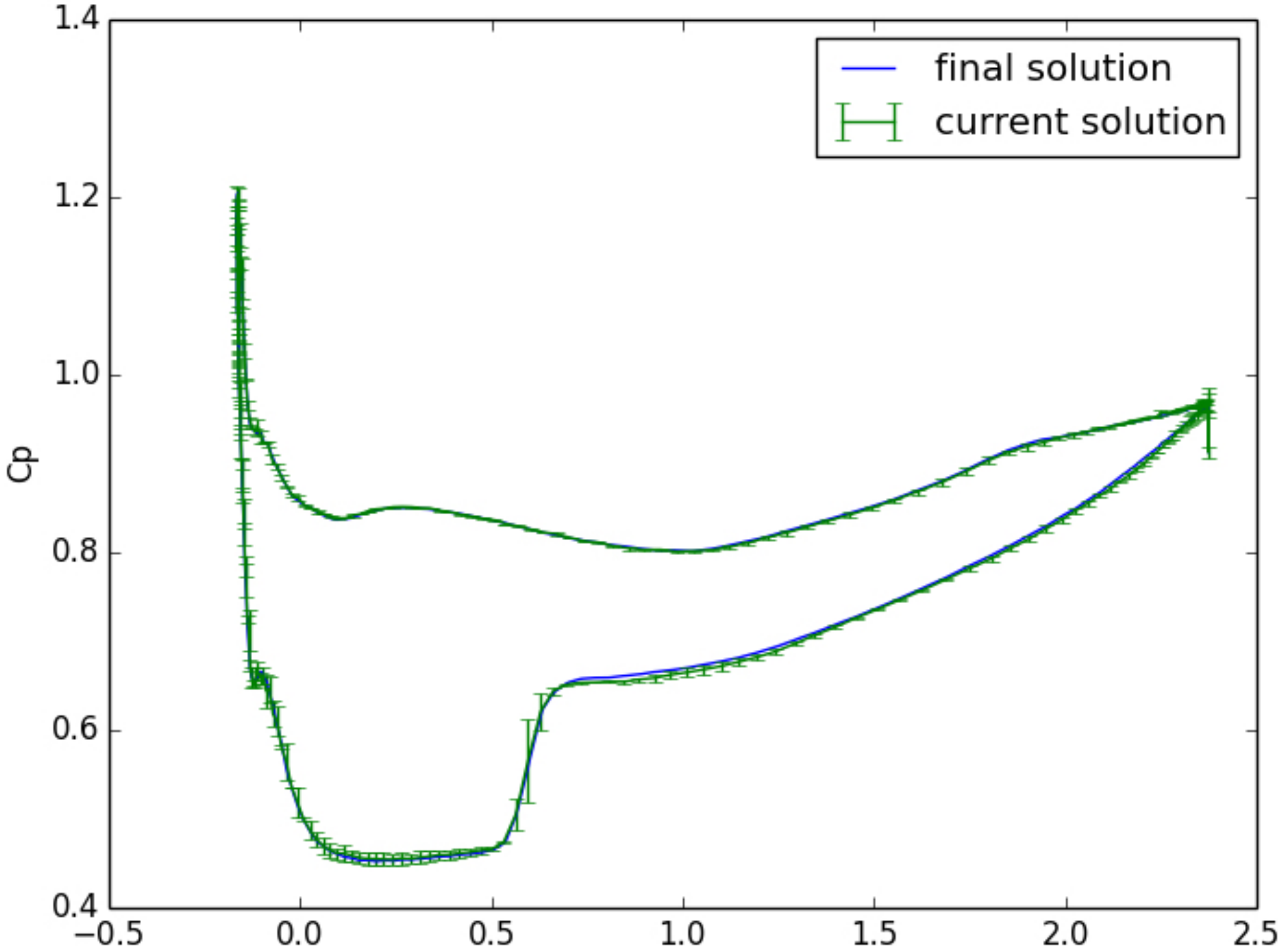
final solution
current solution
Cp
1.4
1.2
1.0
0.8
0.6
0.4
−0.5
0.0
0.5
1.0
1.5
2.0
2.5

Higher order (and unsteady) approximations

Central Essentially Non Oscillating (T. Barth, C. Groth)

Vertex, dual cell, 2-exact quadratic reconstruction

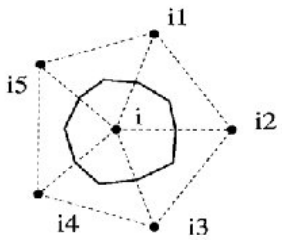

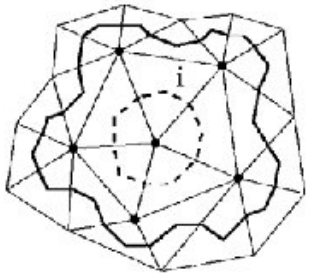

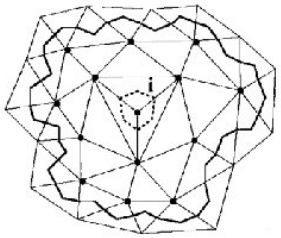

Given $\bar{u}_i$ $\forall$ cell i of centroid G_i, find the $c_{i,\alpha}$, $|\alpha| \leq \mathbf{2}$ s.t.:

$$R_2^0 \bar{u}_i(x) = \bar{u}_i + \sum_{|\alpha| \leq 2} c_{i,\alpha} [(X - G_i)^\alpha - \int_{Cell_i} (X - G_i)^\alpha \mathrm{d}\mathbf{x}]$$

$$\overline{R_2^0 \bar{u}} = \int_{Cell_i} R_2^0 \bar{u}_{i,i} \mathrm{d}\mathbf{x} = \overline{u_i}$$

$$\sum_{j \in N(i)} (\overline{R_2^0 \bar{u}_{i,j}} - \overline{u_j})^2 = Min \ .$$

Reconstruction error analysis (2)

Same treatment as interpolation

R_2: 2D quadratic ENO reconstruction:

$$|u(\mathbf{x}) - R_2^0 u(\mathbf{x})| \approx |\sum_{i=0}^{i=3} \binom{k}{i} a_i x^i y^{k-i}| \leqslant \left(|D_3 u(\delta \mathbf{x})^3|\right)$$

$a(u)_i$ are third derivatives of u.

CENO2 Scheme (1)

Variational statement of the Euler model

$$B(u,v) = \int_\Omega v\nabla\cdot\mathscr{F}(u)\,\mathrm{d}\Omega - \int_\Gamma v\mathscr{F}_\Gamma(u)\,\mathrm{d}\Gamma,$$

B is linear with respect to v.

Find $u \in \mathscr{V}$ such that $B(u,v) = 0\ \forall\ v \in \mathscr{V}$.

CENO discrete statement (after C. Groth), vertex version

$$\mathscr{V}_0 = \{v_0, V_0|_{\mathbf{Cell_i}} = const\ \forall\ i\ \mathbf{vertex}\}$$

Find $u_0 \in \mathscr{V}_0$ such that $B(R_2^0 u_0, v_0) = 0\ \forall\ v_0 \in \mathscr{V}_0$

CENO2 Scheme (2)

2-exact flux integration

The integral on a cell interface $C_{ij} = C_i \cap C_j$ is split into the integrals on the two segments of C_{ij}.

On each segment $C_{ij}^{(1)}$ and $C_{ij}^{(2)}$ a numerical integration with two Gauss points (two Riemann solvers) is applied.

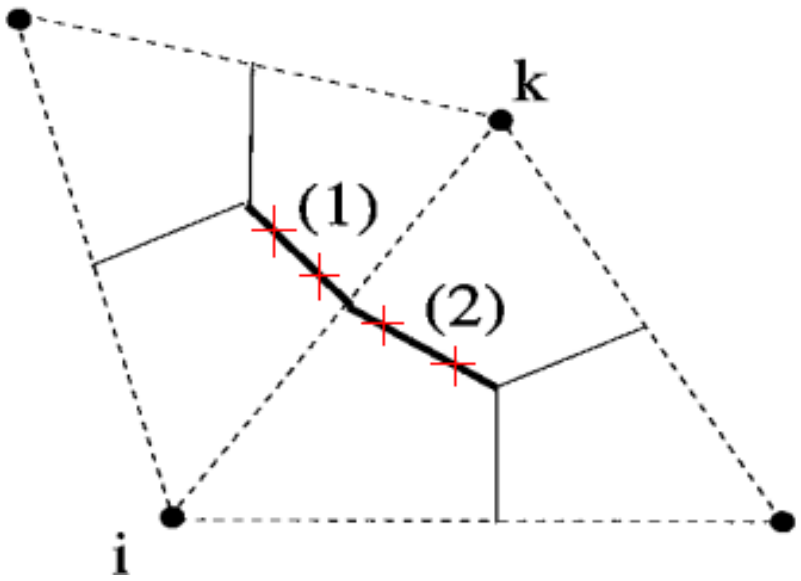

A priori error analysis (1)

Scalar output $\quad j(u) = (g, u).$

Projection π_0: $\mathscr{V} \to \mathscr{V}_0,\ v \mapsto \pi_0 v$

$$\forall\ C_i, \text{dual cell}, \quad \pi_0 v|_{C_i} = \int_{C_i} v dx / meas(C_i).$$

Output error $\quad \delta j = (g, R_2^0 \pi_0 u - R_2^0 u_0).$

The adjoint state $u_0^* \in \mathscr{V}_0$ is the solution of:

$$\frac{\partial B}{\partial u}(R_2^0 u_0)(R_2^0 v_0, u_0^*) = (g, R_2^0 v_0),\ \forall\ v_0 \in \mathscr{V}_0.$$

A priori error analysis (2)

Simpler case:

$B(u,v) = F(v)$ where B is bilinear, F is linear, for example:
$B(u,v) = \int_\Omega v div(\mathbf{V}u)\mathrm{d}\Omega + \int_\Gamma uv\mathbf{V}\cdot\mathbf{n}\mathrm{d}\Gamma$ and
$F(v) = \int_\Gamma u_B v\mathbf{V}\cdot\mathbf{n}\mathrm{d}\Gamma$.

$$\begin{aligned} B(R_2^0 u_0, v) &= F(v) \quad \text{(discrete state eq.)} \\ B(v, u_0^*) &= (g, v) \quad \text{(discrete adjoint. eq.)} \end{aligned}$$

Simpler case (cont'd):

$\Rightarrow$

$$
\begin{aligned}
&(g, R_2^0\pi_0 u - R_2^0 u_0) = \\
&B(R_2^0\pi_0 u - R_2^0 u_0, u_0^*) \quad \text{(discr.adj. eq.)} \\
&= B(R_2^0\pi_0 u, u_0^*) - B(R_2^0 u_0, u_0^*) \\
&\approx B(R_2^0\pi_0 u, u_0^*) - F(u_0^*) \quad \text{(discr.state eq.)} \\
&\approx B(R_2^0\pi_0 u, u_0^*) - B(u, u_0^*) \quad \text{(cont.state eq.)} \\
&\approx B(R_2^0\pi_0 u - u, u_0^*)
\end{aligned}
$$

A priori error analysis (3)

Unsteady Euler: $W = (\rho, \rho u, \rho v, \rho E)$

For the case of Euler eqs, we get after some calculations:

$$|B(R_2^0 \pi_0 W - W, W_0^*)| \approx \leq$$
$$2 \int_\Omega \sum_q K_q(W, W^*) |R_2^0 \pi_0 u_q - u_q| \, \mathrm{d}\Omega$$

with $(u_q)_{q=1,8} = (W, W_t)$,
and in which the $K_q(W, W^*)$ are built from space derivatives of W^* and Euler fluxes derivatives with respect to dependant variable W.

Optimal metric (1)

$$|R_2^0 \pi_0 u_q - u_q| \approx \left(|D_3 u_q (\delta \mathbf{x})^3|\right) \ .$$

Third derivatives are evaluated by reconstruction.

An equivalent pseudo-Hessian S_q is computed by a **least square fitting** on the neighboring cells j:

$$S_{q,i} \ = \ Argmin \sum_{j=1}^{N(i)} \left(\ S_{q,i}(\overrightarrow{\mathbf{ij}})^2 \ - \ (|(D_3 u_q)_i (\overrightarrow{\mathbf{ij}})^3|)^{2/3} \ \right)^2$$

$$|R_2^0 \pi_0 u_q - u_q| \approx \left(trace(\mathscr{M}^{-1/2} S_q \mathscr{M}^{-1/2}) \right)^{\frac{3}{2}} \ .$$

Optimal metric (2)

Optimization problem

Minimize :

$$\mathscr{E} = \int \sum_q K_q(W, W^*) \left(trace(\mathscr{M}^{-1/2} S_q \mathscr{M}^{-1/2}) \right)^{\frac{3}{2}} dxdy$$

$$= \int \left(trace(\mathscr{M}^{-1/2} S \mathscr{M}^{-1/2}) \right)^{\frac{3}{2}} dxdy$$

with constraint $\int d_{\mathscr{M}}\, dxdy = N$.

$$\Leftrightarrow \mathscr{M}_{opt} = N \left(\int det(S)^{\frac{3}{5}}\, dxdy \right)^{-1} det(S)^{-\frac{2}{5}}\, \mathscr{R}_S \bar{\Lambda}_S^{-1} \mathscr{R}_S^T$$

Unsteady mesh adaptation: Global fixed point

- The time interval is divided in n_{adap} *sub-intervals* in which the adapted mesh is frozen.
- The n_{adap}-uple $\left(\mathscr{M}_{i_{adap}}, i_{adap} = 1, n_{adap}\right)$ minimizes the total functional error under the constraint of a prescribed total number of vertices.
- The adaptation loop iterates over the whole time interval:
  - Computation of state solution.
  - Computation of adjoint.
  - Evaluation of the n_{adap} metrics.
  - Generation of the n_{adap} unit meshes.

Unsteady mesh adaptation: Global fixed point

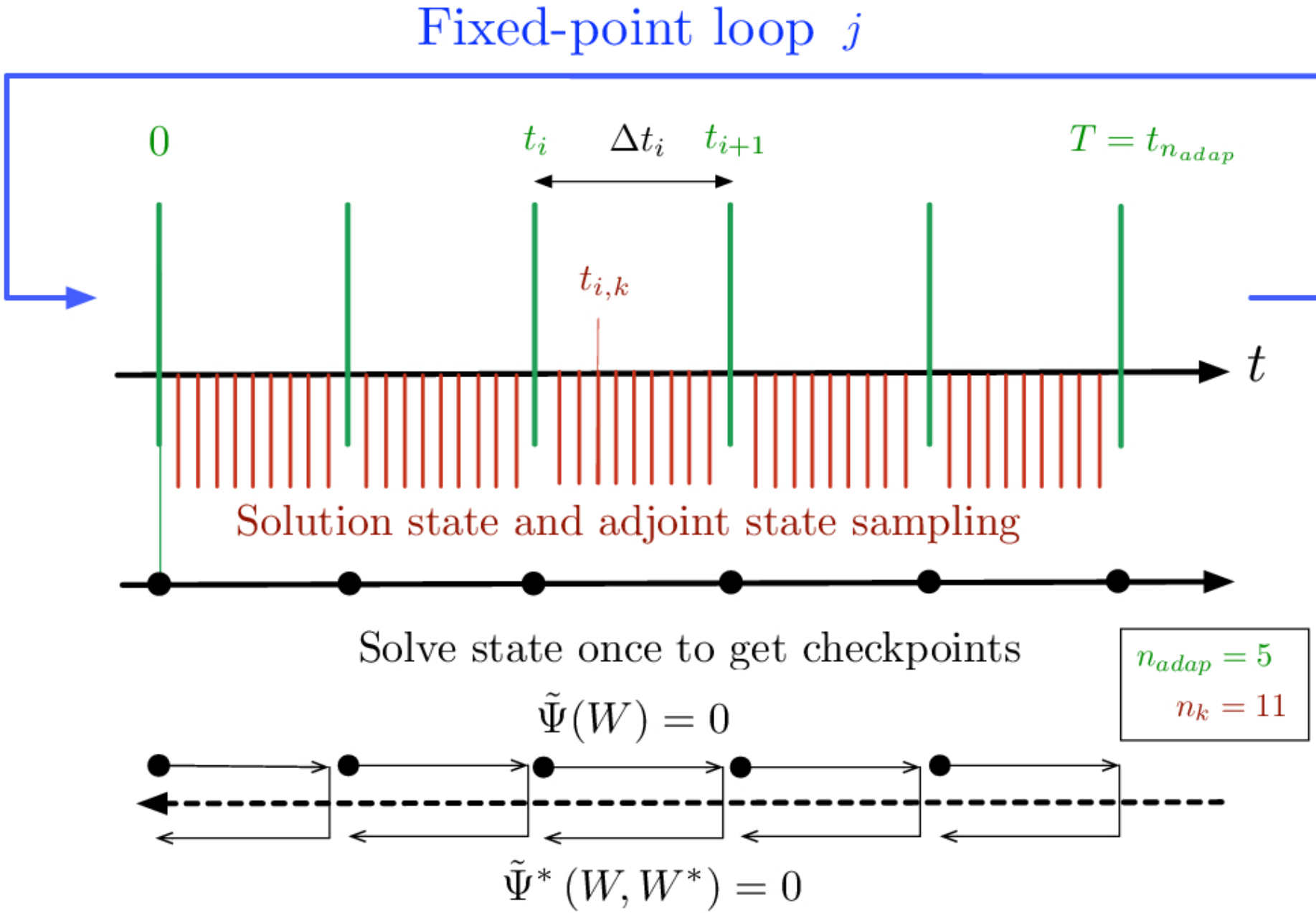

Two numerical examples

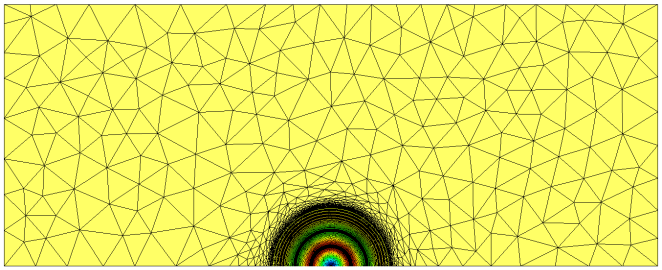

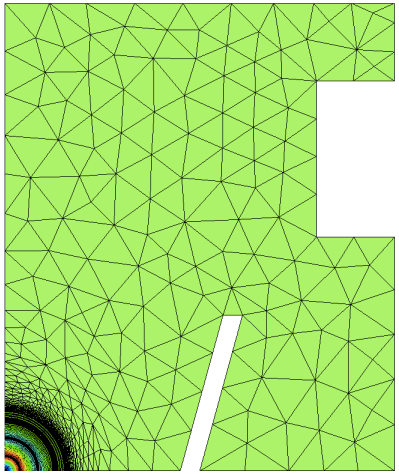

- Nonlinear acoustics (Euler).
- Noise source on “road”, bottom left.
- Case 1: Propagation in a rectangulat box.
- Micro on top center.
- Case 2:Propagation around an anti-noise oblique “wall”.
- Micro on lower part of a “balcony”.
- Output functional = integral of pressure at micro.

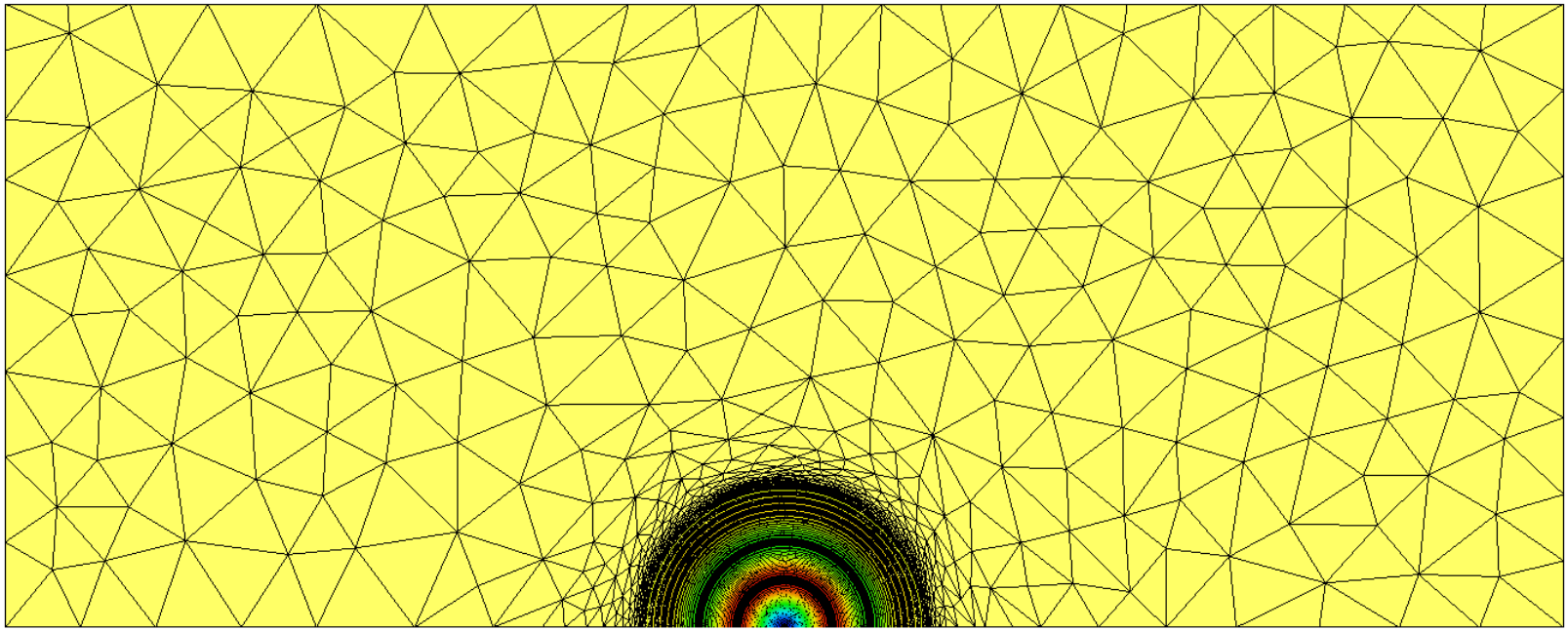

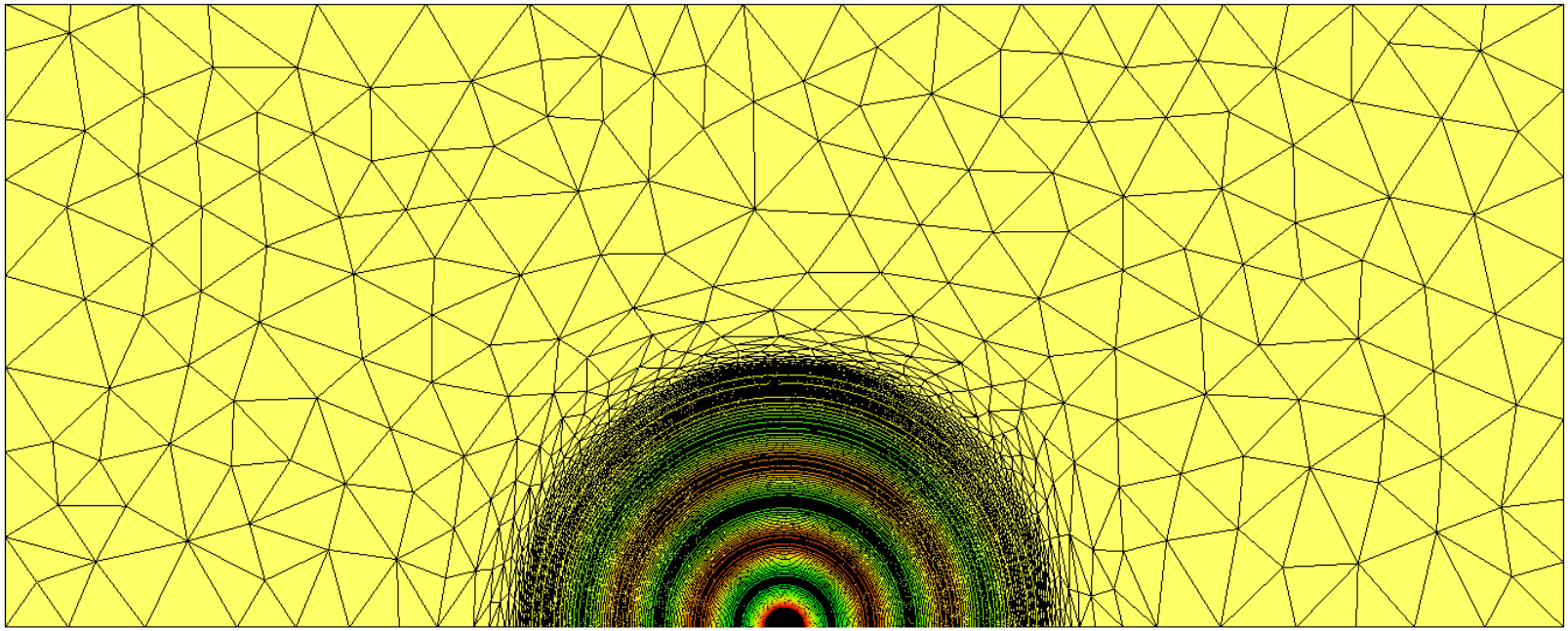

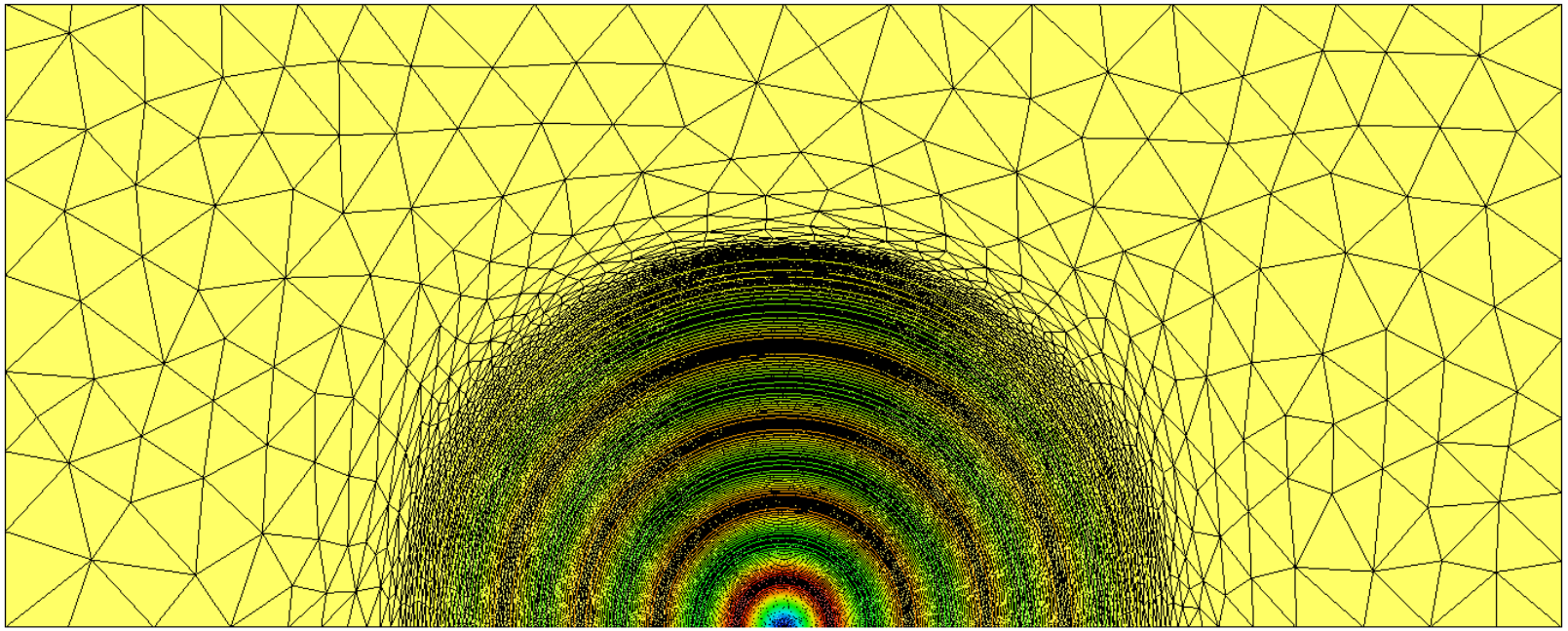

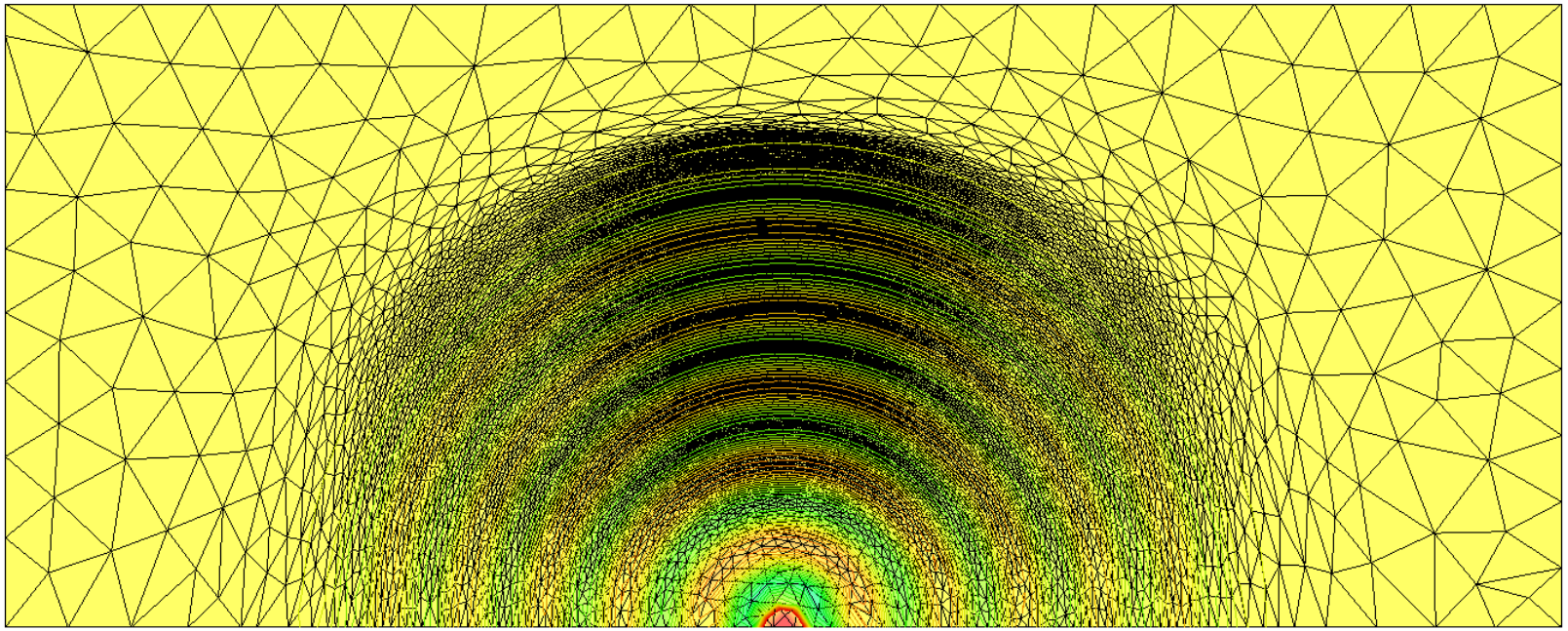

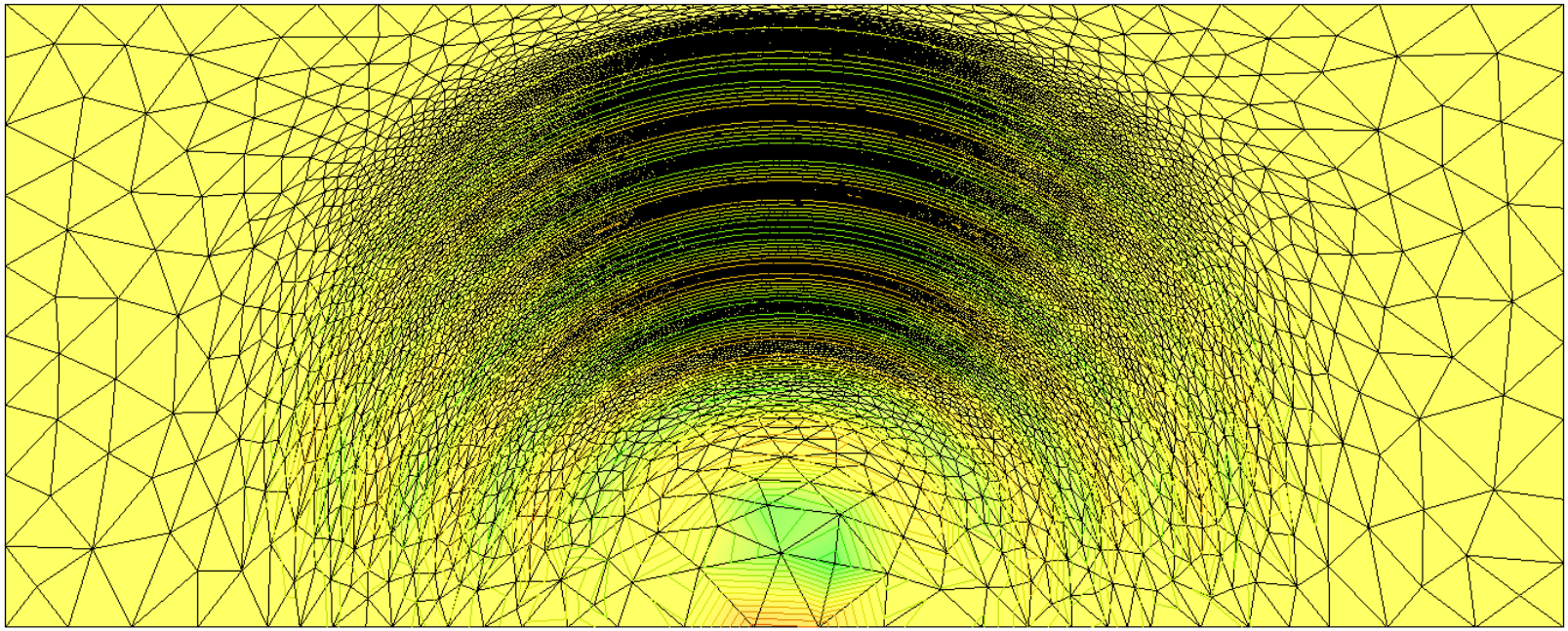

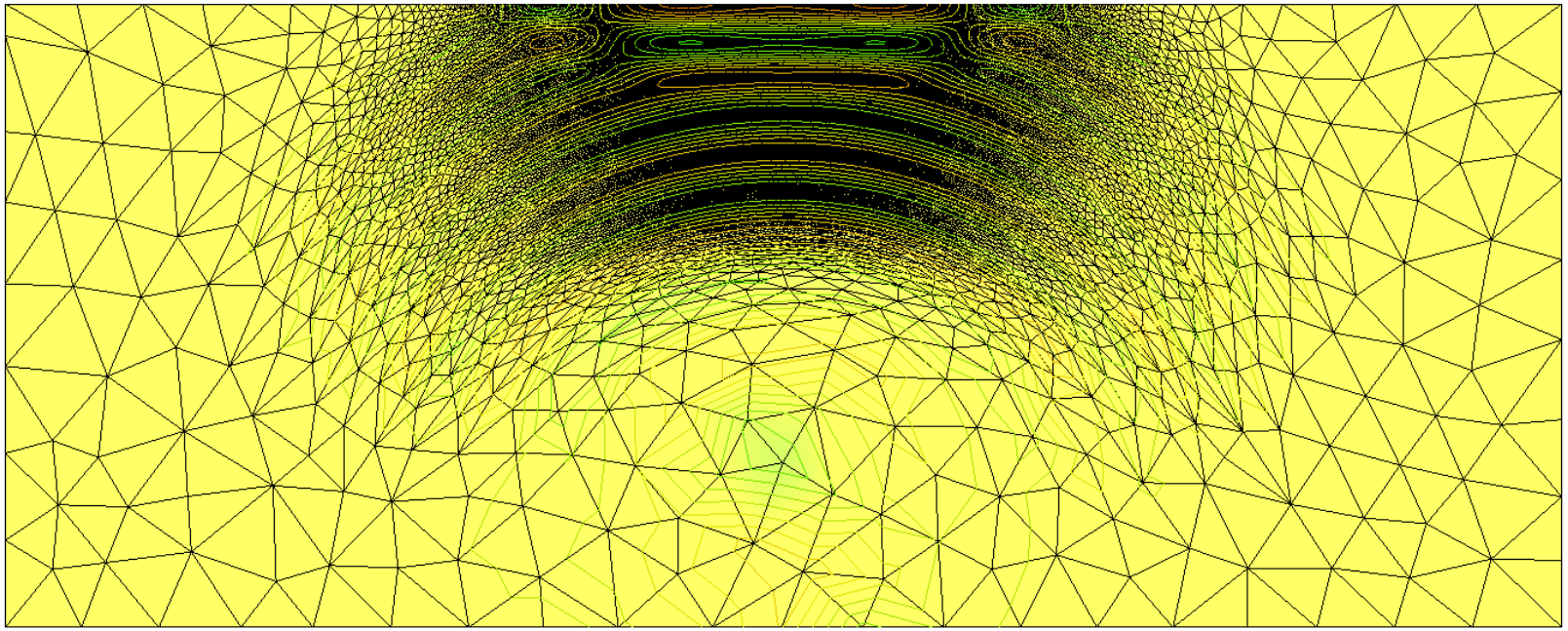

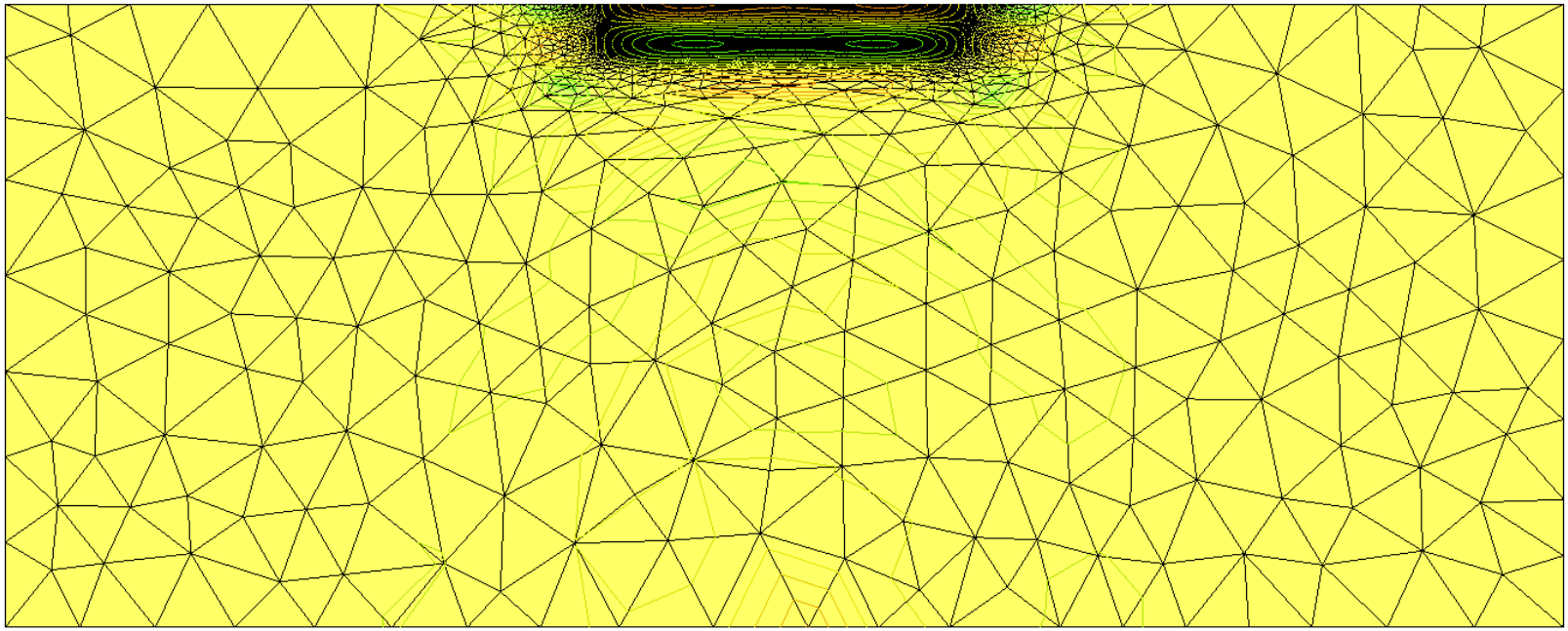

Mean pressure at bottom as a function of time:

Adapted meshes: 2700 vertices in mean, 5400, 10700: **O(2.72)**.

Aspect ratio in refined zone: 3-4.

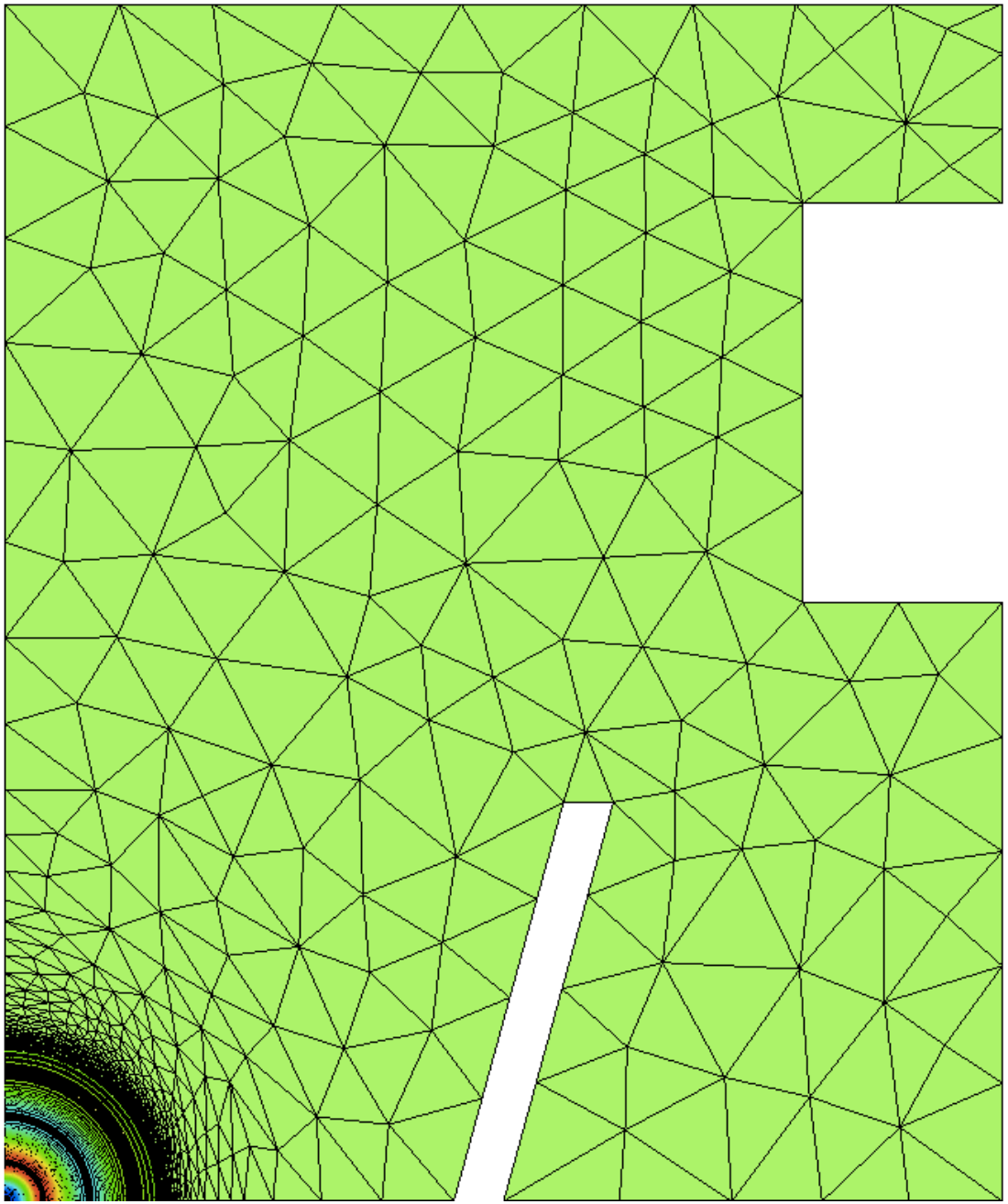

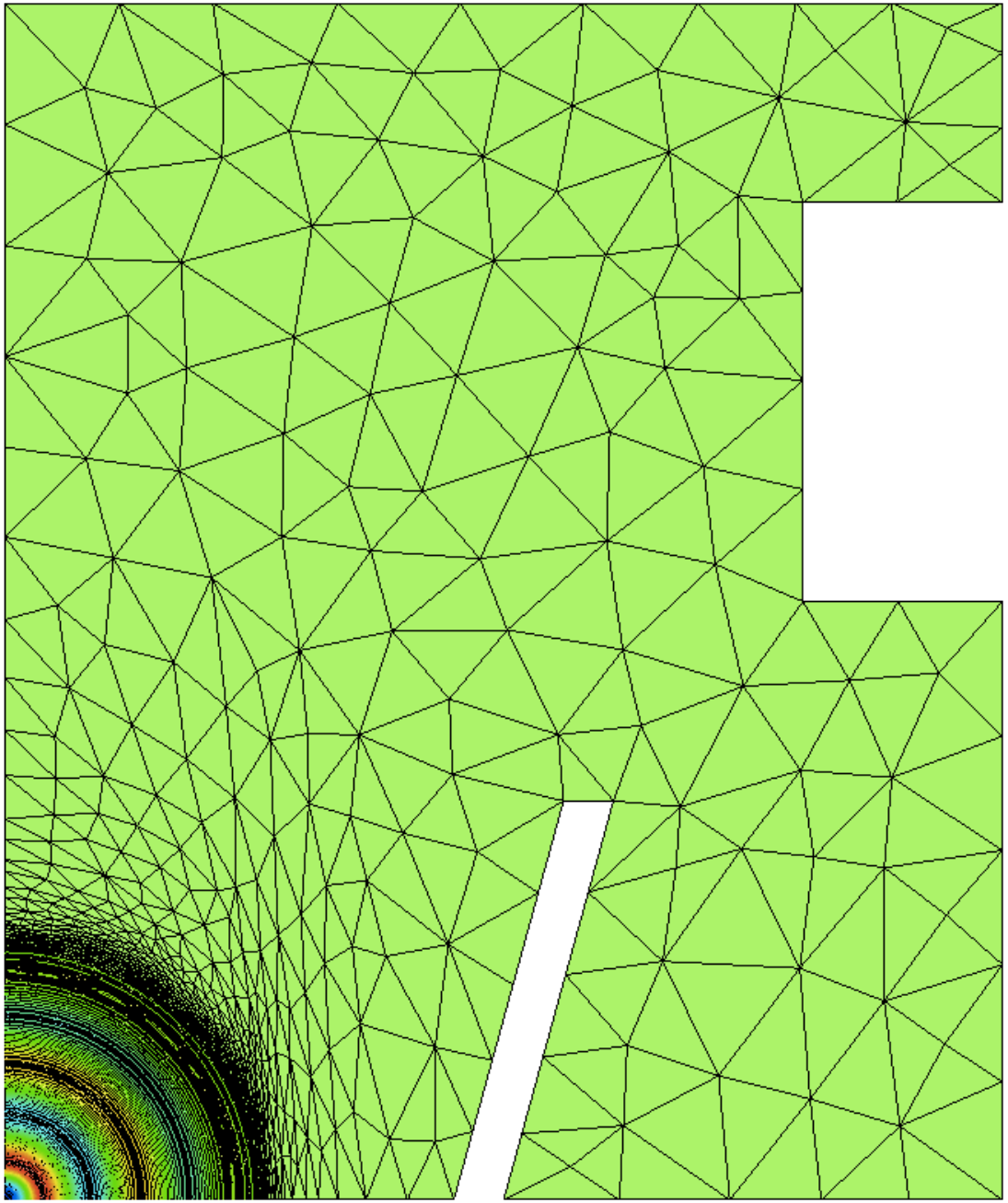

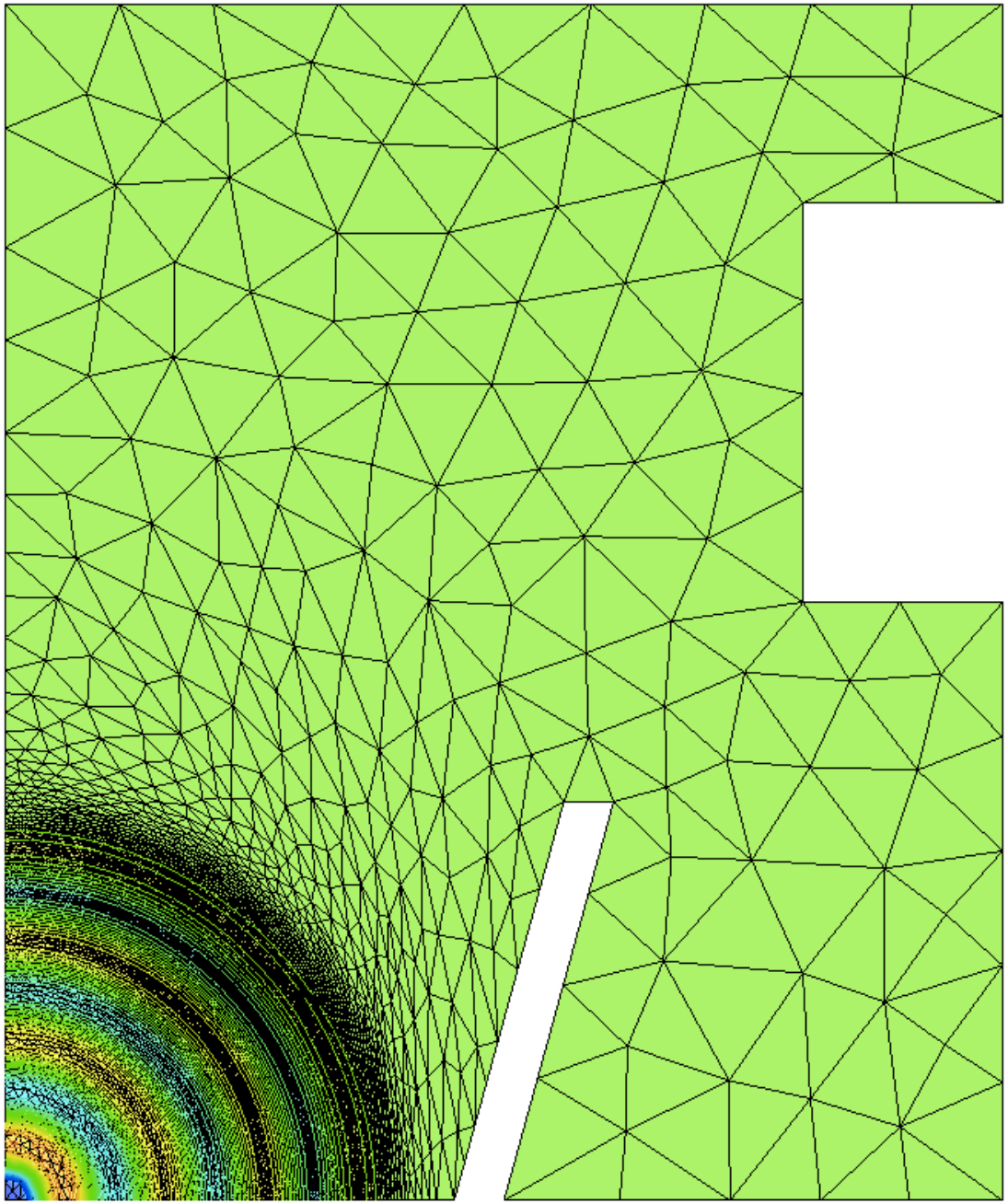

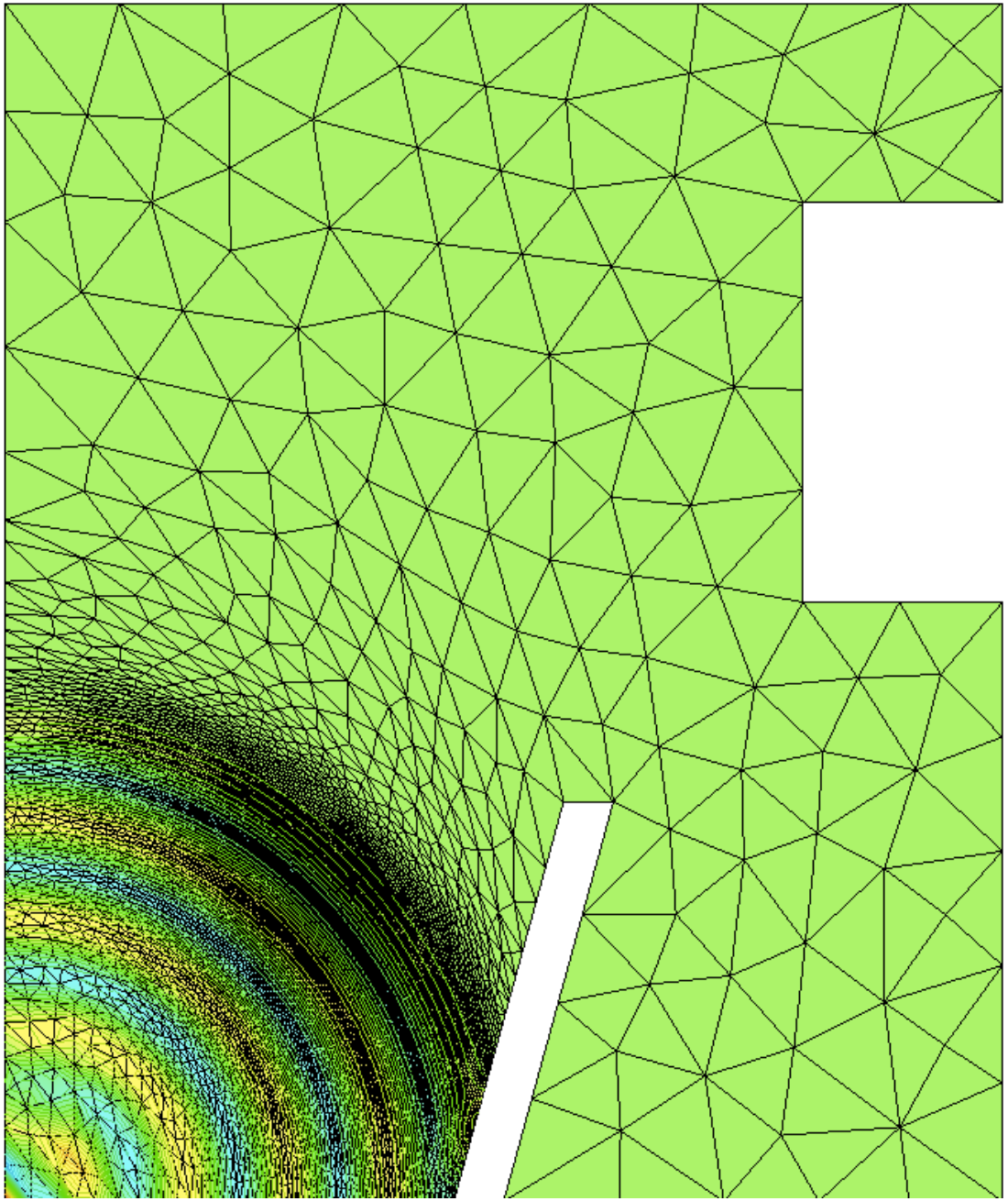

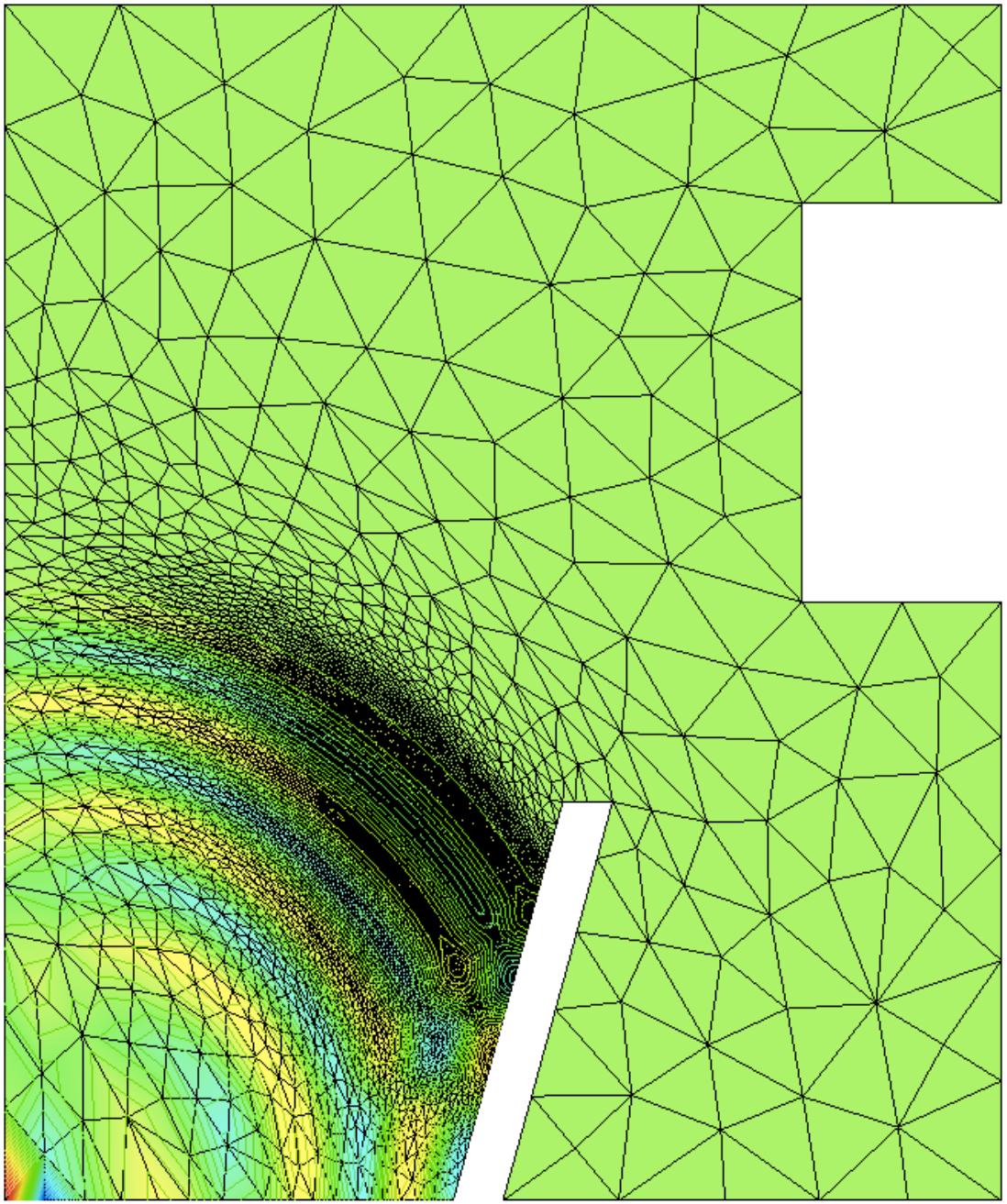

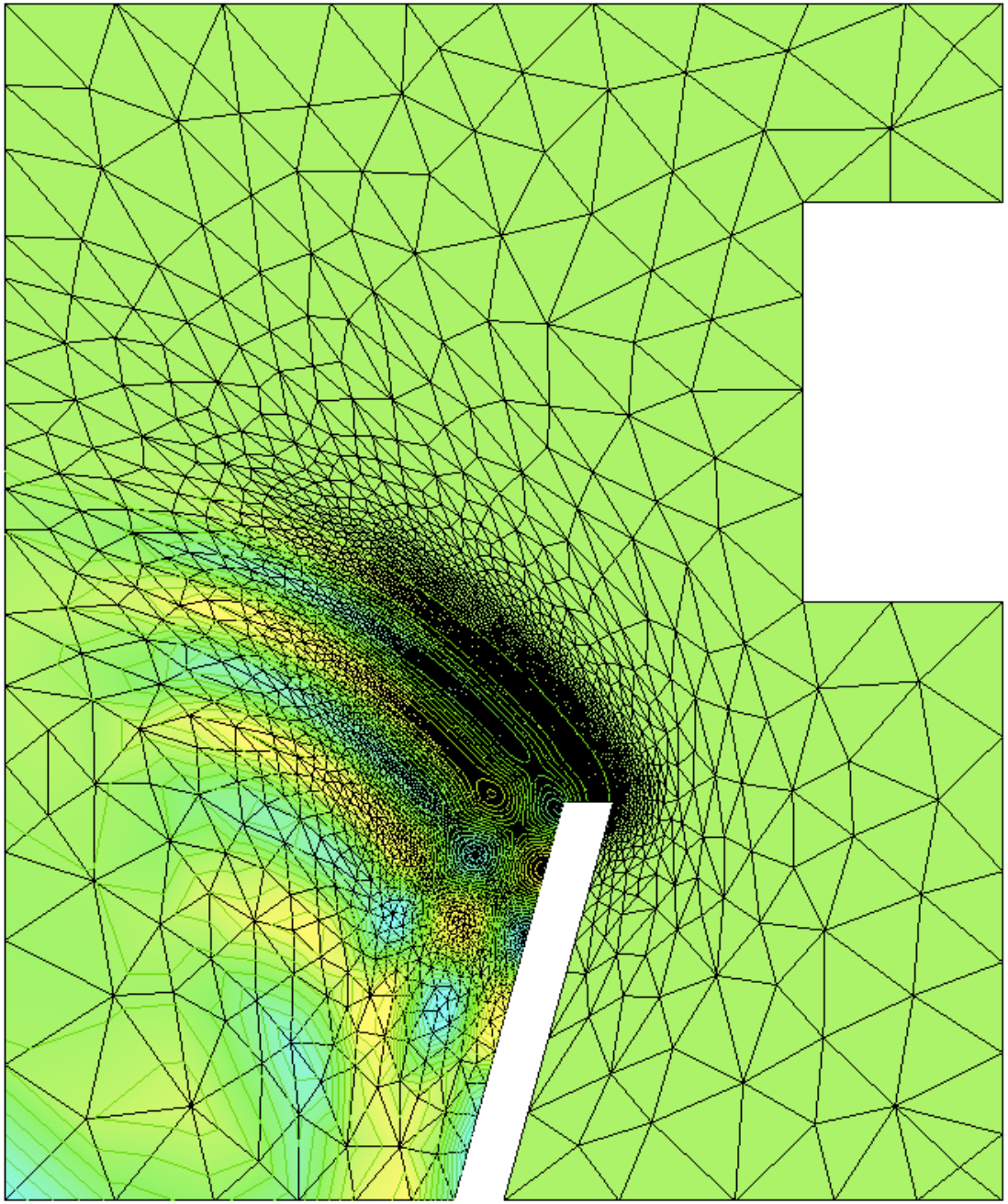

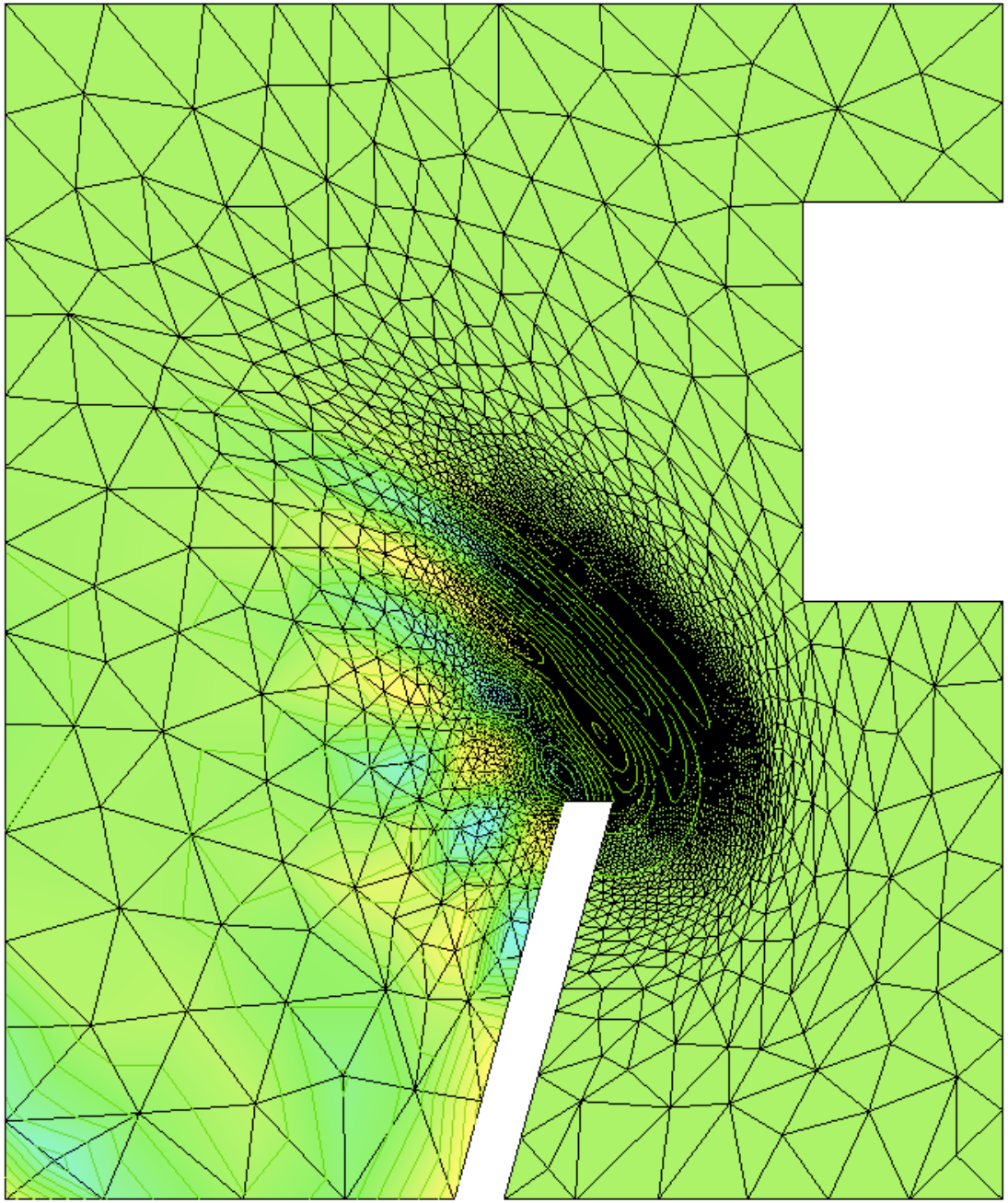

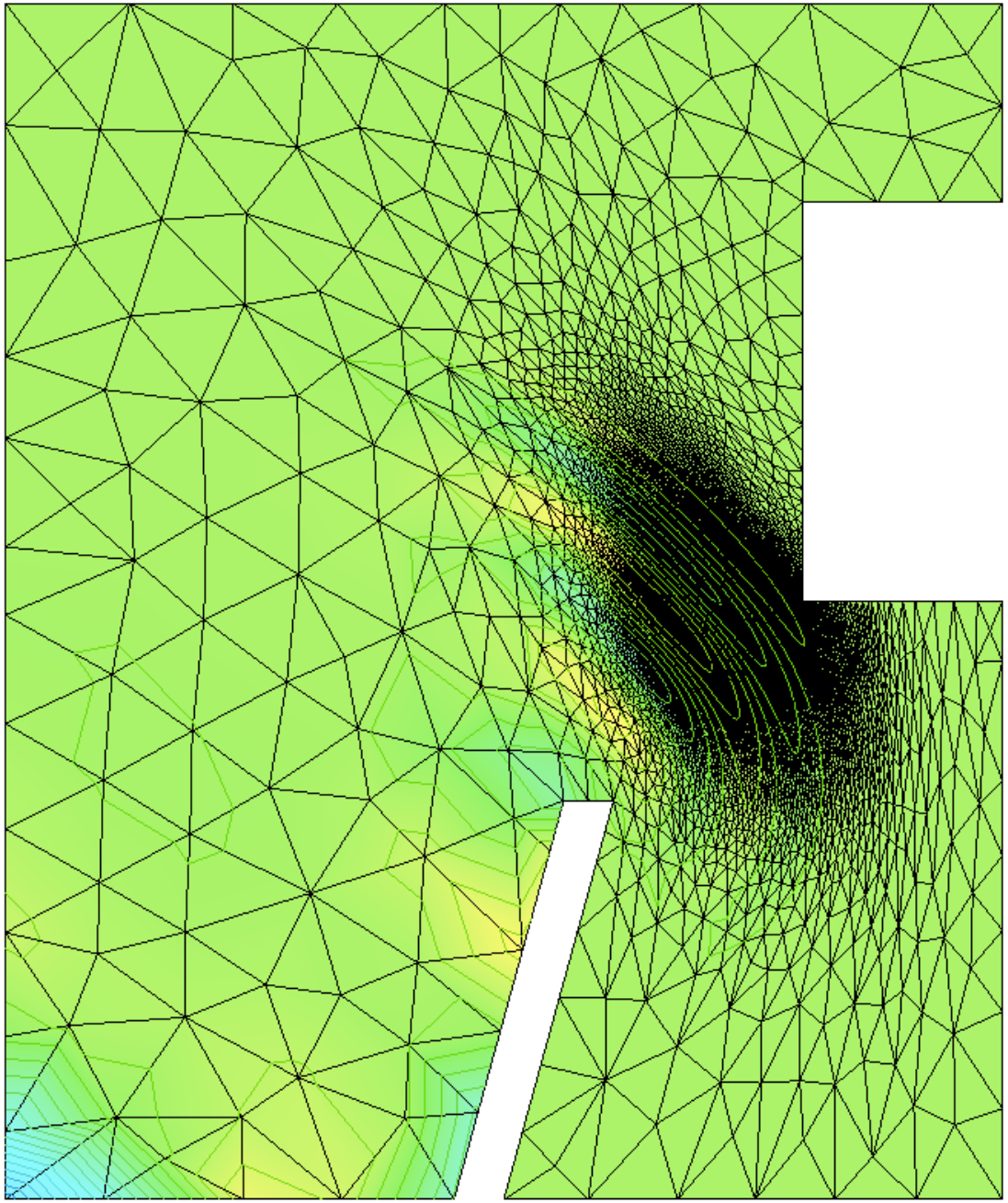

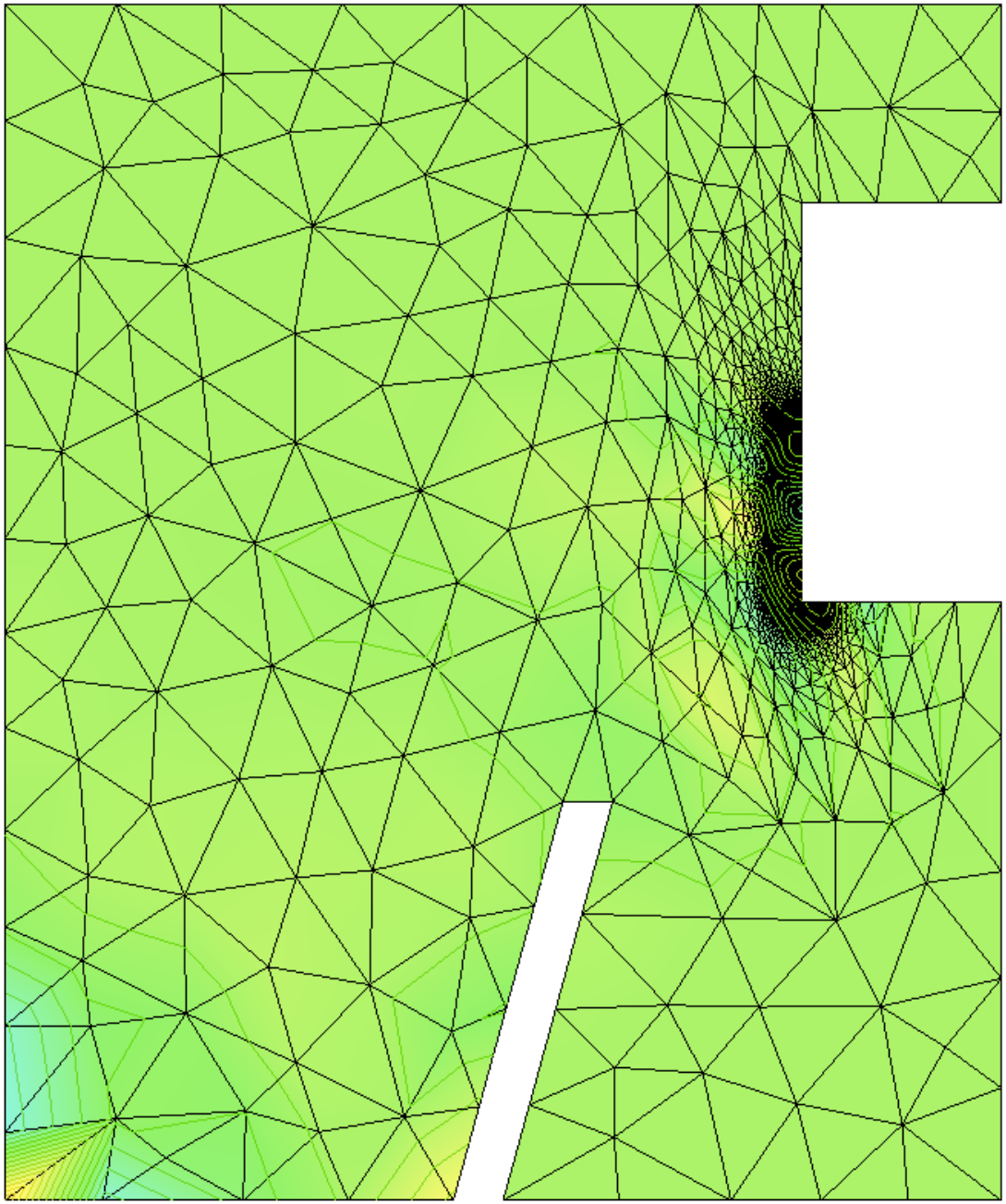

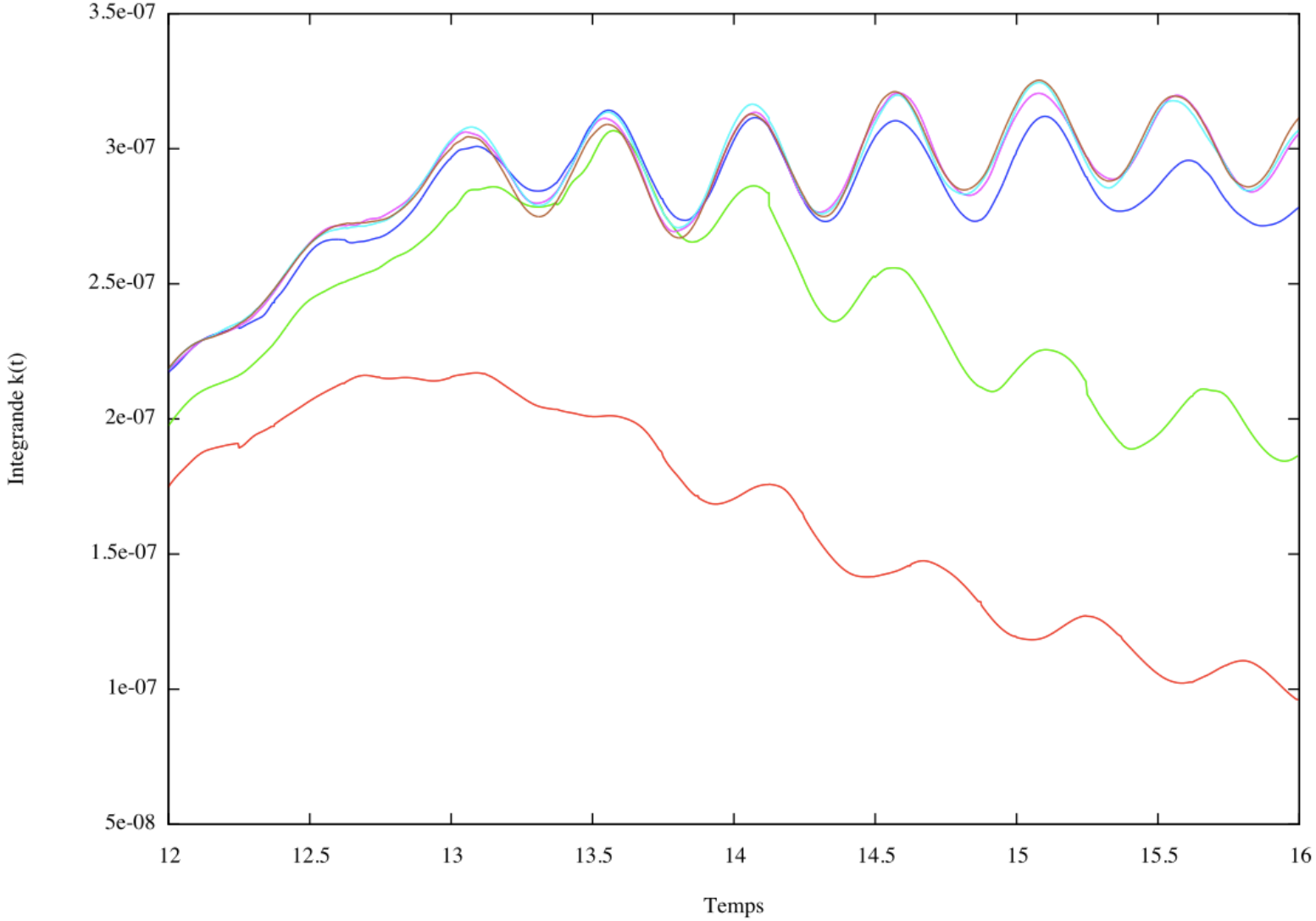

Mean pressure at balcony bottom as a function of time:

-*Uniform* meshes in red(*57K*) and green(*117K*): **O(1)**.

-Adapted meshes: 2K≈*578K*, (8K≈*1.25M*, 15K, 31K≈*5M*): **O(2.48)**.

Aspect ratio in refined zone: 3-4.

About convergence order of unsteady case

- Then space convergence is observed by increasing the mean number of vertices over the n_{adap} meshes.
- Space-time convergence:
  - Needs to add the time error.
  - The discretization parameter n_{adap} needs to be increased.
  - Due to a unique time-step, space-time convergence is limited to 8/5$<$ 2.(*)
  - Pushing higher the 8/5 limit may be obtained with a multi-rate time advancing.

(*)A. Belme, A. Dervieux, F. Alauzet, Time Accurate Anisotropic Goal-Oriented Mesh Adaptation for Unsteady Flows, *J. Comp. Phys.*, 231:19, 2012, 6323-6348

CONCLUSIONS

Anisotropic mesh adaptation can address simulations which are **not** affordable without adaptation.

Anisotropic mesh adaptation carries more surely **O2 mesh convergence** for many types of user-prescribed outputs.

Anisotropic mesh adaptation progressively frees the user from delicate mesh management.

We have illustrated these properties with interpolation-based *a priori* estimates made of many approximations but, at last, rather accurate.

CONCLUSIONS, TO BE IMPROVED

The correctors are useful for adaption purpose but need improvements in order to give an accurate estimate of the approximation error.

CONCLUSIONS, TO BE DONE

The mastering of **high-Reynolds aerodynamics** needs to combine efficiently mesh adaptation with highly stretched meshes.

$$\text{mesh} \mapsto \text{error} \mapsto \text{metric} \mapsto \text{mesh}$$

This needs in particular to improve:

- discrete error evaluation,
- mesh generation.

For **space-time O2/O3** unsteady calculations, still a long way has to be gone.